THE STUDY OF HUMAN WEIGHT ON THE BIOMECHANICAL BEHAVIOUR OF INTERVERTEBRAL DISC USING FINITE ELEMENT ANALYSIS

YEW JUNSIN

UNIVERSITI TEKNIKAL MALAYSIA MELAKA

THE STUDY OF HUMAN WEIGHT ON THE BIOMECHANICAL BEHAVIOUR OF INTERVERTEBRAL DISC USING FINITE ELEMENT ANALYSIS

YEW JUNSIN

This report is submitted in fulfillment of the requirements for the degree of Bachelor of Mechanical Engineering

Faculty of Mechanical Engineering

UNIVERSITI TEKNIKAL MALAYSIA MELAKA

2019

DECLARATION

I declare that this project report entitled "The study of human weight on the biomechanical behaviour of intervertebral disc using finite element analysis" is the result of my own work except as cited in the references.

Signature	:	....
Name	:	....
Date	:	....

APPROVAL

I hereby declare that I have read this project report and in my opinion this report is sufficient in terms of scope and quality for the award of the degree of Bachelor of Mechanical Engineering.

Signature :. ....

Name of Supervisor : ....

Date : ....

DEDICATION

This thesis is wholeheartedly dedicated to my beloved parents and family, who have been my source of inspiration and constantly provided me with moral, spiritual, emotional and financial support. This is also dedicated to my respectful supervisor for his mentorship throughout this study. Lastly, to my friends who shared their words of advice and encouragement to finish this study.

ABSTRACT

Obesity is a growing healthcare issue, which always associated with different kind of diseases, such as hypertension, osteoarthritis (OA), intervertebral disc degeneration, body pain and difficulty in physical functioning. Excessive load on the spine could change the mechanical behaviour of the lumbar spine and affect the pressure and stress that occurs in the intervertebral disc particularly at nucleus pulposus and annulus fibrosus. However, the biomechanical effects of body weight on the lumbar spine are yet to be fully understood. Thus, the purpose of this study was to investigate the biomechanical effects of body weight on the lumbar spine. Finite element analysis (FEA) is a suitable method in the study of intervertebral disc since it can provide a FE model for repeated simulation, which can greatly save the time consuming and more cost-efficient. The finite element model was subjected to follower compression load of 700 N, 900 N and 1300 N to represent the load case of normal, overweight and obese with a combination of pure moments of 7.5 Nm in flexion. Increasing weight shows significant effect on the kinematics of the lumbar spine for both finite element models. The excessive load on the lumbar spine increased the pressure and stress that occurs in the intervertebral disc, particularly at the nucleus pulposus and annulus fibrosus. The nucleus pressure was higher in flexion and increased as the compressive load was increased. This phenomenon could contribute to the earliest stages of disc degeneration, which occurs in the nucleus pulposus. In conclusion, flexion increases the nucleus pressure and appears to have differing affects to disc structure. Heavier individuals are expected to experience an increase in stress and pressure of the disc regardless of the position of the spine. Therefore, an increase in body weight of the lumbar spines changed the kinematics of the lumbar spine and causes an increase in the nucleus pressure and annulus stress. This may be a factor that can lead to early intervertebral disc damage particularly at disc rim.

ABSTRAK

Obesiti adalah satu isu kesihatan yang semakin meningkat dan ia selalu dikaitkan dengan pelbagai jenis penyakit seperti tekanan darah tinggi, osteoartritis (OA), penyakit cakera degenatif, sakit badan dan kesukaran dalam fungsi fizikal. Beban yang dikenakan pada tulang belakang boleh mengubah tindak balas mekanikal tulang belakang dan menjejaskan tekanan kepada cekera intervertebral terutamanya pada nukleus pulposus dan anulus fibrosus. Walau bagaimanapun, kesan berat badan pada tulang belakang lumbar secara biomekanik masih belum difahami sepenuhnya. Oleh itu, tujuan kajian ini dibuat adalah untuk mengkaji kesan biomekanik berat badan pada tulang belakang lumbar. Analisis unsur terhingga (FEA) adalah satu kaedah yang sesuai dalam kajian cekera intervertebral kerana FEA boleh menyediakan model FE yang boleh digunakan dalam simulasi berulang dan membantu dalam menjimatkan masa dan kos. Beban mampatan secara ikutan iaitu 700 N, 900 N dan 1300 N dikenakan kepada model-model unsur terhingga untuk mewakili kes beban berat badan yang normal, berlebihan dan obes, dengan gabungan momen tulen sebanyak 7.5 Nm dalam akhiran. Peningkatan berat badan telah menunjukkan kesan yang ketara ke atas kinematik tulang belakang lumbar untuk kedua-dua model tiga dimensi unsur terhingga. Beban yang berlebihan pada tulang belakang lumbar meningkatkan tekanan yang berlaku dalam cakera intervertebral terutamanya di nukleus pulposus dan anulus fibrosus. Tekanan nukleus adalah lebih tinggi pada pergerakan akhiran dan meningkat apabila beban mampatan yang dikenakan meningkat. Fenomena ini boleh menyebabkan berlakunya kemerosotan pada cakera di peringkat paling awal di mana ianya berlaku pada nukleus. Kesimpulannya, pergerakan lanjutan meningkatkan tekanan pada annulus dan kesan struktur cakera yang berbeza yang ditunjukkan pada pergerakan akhiran. Individu yang lebih berat dijangka akan mengalami peningkatan dalam tekanan pada cakera tanpa mengira kedudukan tulang belakang. Oleh itu, kenaikan berat badan pada tulang belakang lumbar telah mengubah kinematik tulang belakang lumbar dan ini menyebabkan peningkatan tekanan nukleus dan tekanan anulus. Ini boleh menjadi faktor yang membawa kepada kerosakan awal pada cakera intervertebral terutamanya pada rim cakera.

ACKNOWLEDGEMENT

I would like to express my deepest appreciation to my supervisor Prof Madya Dr Mohd Juzaila Bin Abd Latif for his guidance, advices and support throughout this project. I would also like to take this opportunity to thank UTeM, especially Faculty of Mechanical Engineering for the support of facilities and utilities. I would like to thank my course mates for giving me their support, patience and encouragement. Finally, I would like to thank my family for their support.

TABLE OF CONTENTS

LIST OF FIGURES

LIST OF TABLES

LIST OF ABBEREVATIONS

AF	Annulus fibrosus
ALL	Anterior longitudinal ligament
CL	Facet joint capsule
DDD	Degenerative disc disease
FE	Finite element
FEA	Finite element analysis
FEM	Finite element method
FSU	Functional spinal unit
IDP	Intradiscal pressure
ISL	Interspinous ligament
IVD	Intervertebral disc
LBP	Low back pain
LF	Flaval ligament
L1	The first lumbar vertebra
L2	The second lumbar vertebra
L3	The third lumbar vertebra
L4	The fourth lumbar vertebra
L5	The fifth lumbar vertebra
NP	Nucleus pulposus
PLL	Posterior longitudinal ligament
ROM	Range of motion
SSL	Supraspinous ligament

TDR	Total disc replacement
TL	Intertransverse ligament
VMS	Von Mises stress

CHAPTER 1

INTRODUCTION

1.1 Background

Low back pain (LBP) is a common symptom, occuring in all age groups, from children to the elderly. LBP brings difficulties to human and affects their quality of life and work, which indirectly caused a great socioeconomic burden to the patients and also society (Manchikanti et al., 2014). It is an ordinary condition that drives individuals to search for remedial treatments (Karppinen et al., 2011).

The main cause of LBP is the natural deterioration of an intervertebral disc (IVD), called degenerative disc disease (DDD) (Abi-Hanna et al., 2018). There are many factors that increased the risk of having LBP in the aspects of psychological, social, biophysical, comorbidities and pain-processing mechanisms such as sitting position, prolonged sitting, obesity, aging and smoking. Prolonged activation of the muscle while sitting may also result in muscle fatigue, in which the mechanical stress on ligaments and intervertebral discs is also increased (Granata et al., 2004).

There were around 34% to 51% of the office workers suffering from LBP within 1 year (Waongenngarm et al., 2018). However, women were the major group to experience LBP among those occupational groups that have been studied, especially nurses where the risk estimated to be in the range of 1.2 to 5.5 (Yassi & Lockhart, 2013). Occupation where men were the majority with a worsen condition of LBP was reported to be construction workers, within the range of 2.3 to 3.0 (Bongert et al., 2004).

Obesity has been recognized as the key factor in radiating LBP regardless in young or adults (Manchikanti et al., 2014). Besides, a study had proved that weight gain led to the increase in the mechanical loading on the lumbar spine, which directly caused a reduction in disc hydration, changed biomechanical and eventually result in disc degeneration and low back pain (Peng et al., 2018). The term ‘disc degeneration’ is a spinal condition involving the natural deterioration of an intervertebral disc such as disc herniation as shown in Figure 1.1 (Abi-Hanna et al., 2018). Disc herniation which also known as disc protrusion or extrusion, led to a focal bulging with 3mm or greater beyond the vertebral margin (Clarencon et al., 2016).

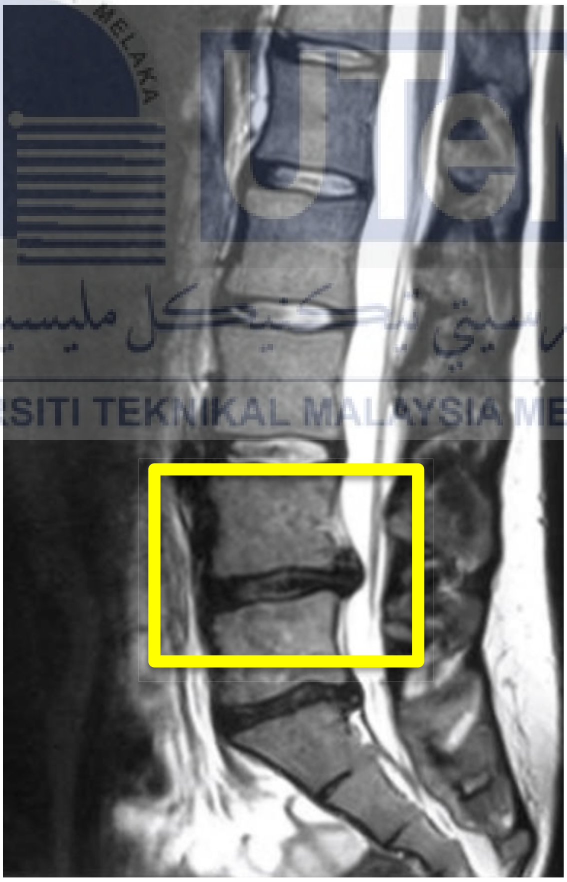

Figure 1.1: Disc herniation in lumbar spine between L4-L5 and L5-S1 (Abi-Hanna et al., 2018).

1.2 Problem statement

Obesity is related to a high prevalence of LBP (Manchikanti et al., 2014). It played a casual role in increasing the mechanical load on the spine, and therefore causing the risk of low back pain (Lake et al., 2000). Extensive studies of the effect of human weight on the biomechanical behavior of IVD have been examined using finite element analysis (FEA). However, some of the researchers used only one component of the IVD in their studies such as only annulus fibrosus was taken into investigation of the degeneration of IVD (Stokes et al., 1987; Iatridis et al., 2005; Karppinen et al., 2011). By using only one component than two components of the IVD will result in different structures and properties.

Besides that, the complete lumbar spine was not considered in some of the studies where only finite element model of a human L4-L5 motion was considered in finite element study (Clarencon et al., 2016; Lee et al., 2016; Bashkuev et al., 2018). It was observed that the whole ligaments were not considered in the study (Hortin et al., 2015). Therefore, this study aims to model the complete lumbar spine including ligaments and nucleus pulposus and annulus fibrosus of IVD.

1.3 Objectives

The objectives of this project are as follows:

1. To improve and verify the finite element model of lumbar spine.
2. To investigate the effects of obesity on the biomechanical behaviour of intervertebral disc.

1.4 Scope of project

The scopes of this project are:

1. To model the ligaments and two parts of IVD, which are the nucleus pulposus and annulus fibrosus, of the current finite element model of lumbar spine using ABAQUS software.
2. To verify the finite element model of the lumbar spine.
3. To examine the stresses of the annulus fibrosus and nucleus pulposus of intervertebral disc at L1-L5 human lumbar spine of different human weight and spine motion.

1.5 General methodology

There are a few methods to be performed in order to achieve this project's objectives. First of all, literature review is important in order to complete this project. Journals, articles and any materials related to the project are gathered from libraries and internet to help readers to understand the information in complete picture.

After collecting information from journals, improvement of finite element model of lumbar spine is performed. The finite element model of the lumbar spine is studied and the model of ligaments is examined to know how it works by using ABAQUS software. The next method used is verification of finite element model to check whether it conforms to its specification. The next step is simulation where the finite element model for normal, overweight and obese weights are made to examine the pressure and stress occurs in the adjacent intervertebral disc.

When simulation is done, analysis and proposed solution is followed. Analysis of the model is interpreted to see the effect of human weight on the biomechanical behaviour of intervertebral disc. Solutions are then proposed according to the analysis. Report writing is the final stage in this methodology where all the information collected is written into a complete report in the final analysis of the project. The methodology used in this study is summed up as shown in the flow chart of Figure 1.2.

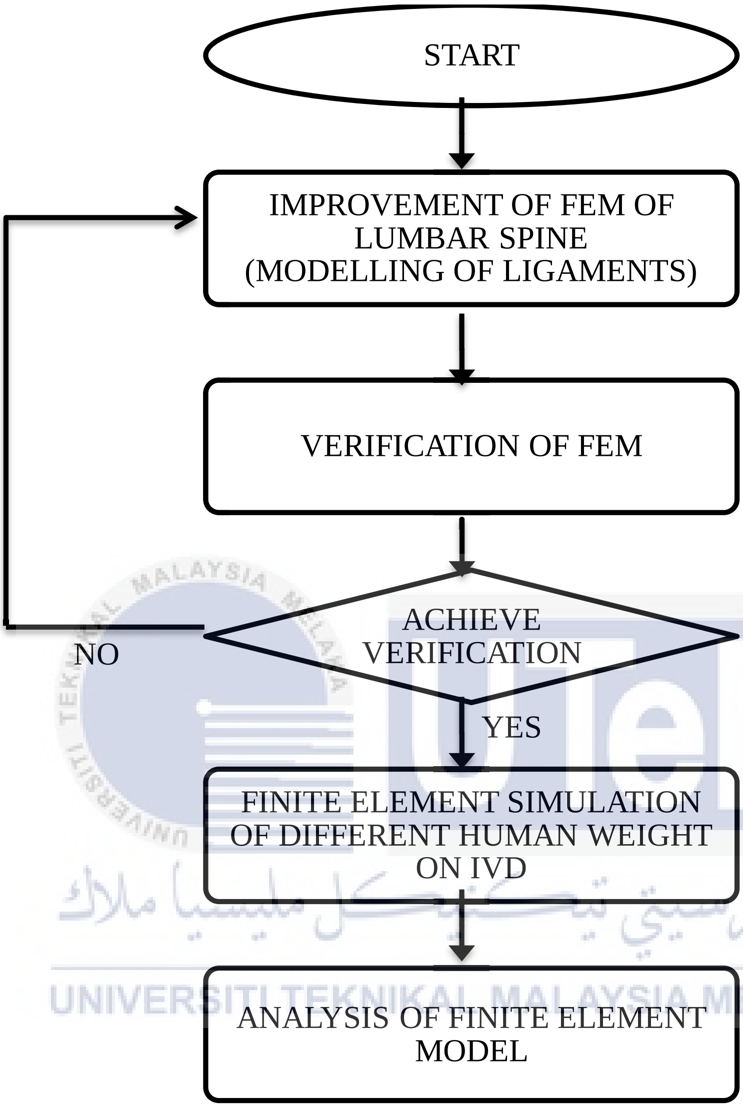

Figure 1.2: Flow chart of the methodology.

CHAPTER 2

LITERATURE REVIEW

2.1 Overview

This chapter studies the background of LBP and human lumbar spine. The finite element (FE) models of the lumbar spine and intervertebral disc are verified and examined for further research. The directions of human body by referring to the anatomic terms are as shown in Figure 2.1.

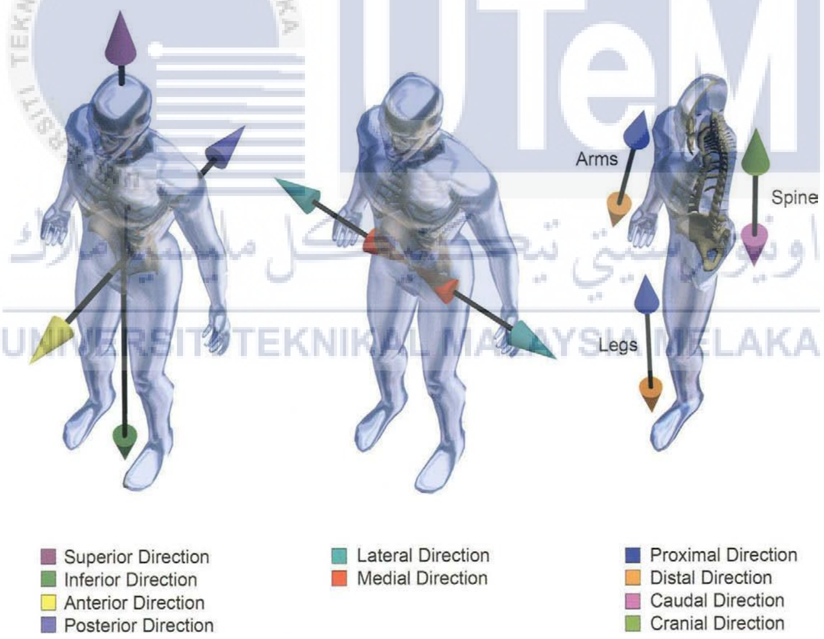

Figure 2.1: Anatomic reference directions (Kurtz and Edidin, 2006).

2.2 Biomechanics of human spine

Biomechanics is important in understanding the contribution of each spinal component to ensure spinal stability. Spinal stability is established by three interlinked components which are the column or passive subsystem, the muscles and tendons or active subsystem, and the central nervous control unit (Izzo et al., 2013). It plays a major role in protecting nervous structures and preventing degeneration of spinal components.

The spine stabilization depends on vertebral architecture and bone mineral density, disc-intervertebral joints, facet joints, ligaments and physiological curves (Oxland et al., 2016). A vertebra may experience fatigue if repetitive loading forces are applied to it. In human spine studies, it is stated that the spinal motion can be classified into 5 mechanisms, which are flexion, extension, axial rotation, lateral bending and traction, as shown in Figure 2.2. The compressive forces acted are based on the curvature of the spine (Friis et al., 2017). Activity such as lifting will cause shear forces to present at each part of the spine as it involves asymmetric loading with respect to the sagittal plane.

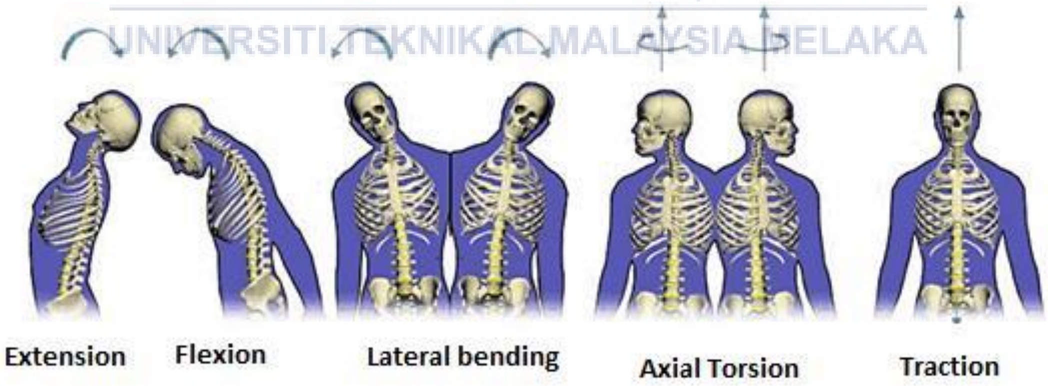

Figure 2.2: Motions of the spine (Kurtz and Edidin, 2006).

2.3 Anatomy of human spine

The spine is a complex structure consisting of components of hard and soft tissue. The vertebrae, which are also known as the bones of the spine are the structure's hard elements (Kurtz & Edidin, 2006). The spine is a significant segment in human body as it acts as a spinal cord protector to support substantial loads and provides the mechanical connection between upper and lower limbs so that movement is allowed in all three planes (Guidi et al., 1994).

The spine consists of 33 vertebrae structurally divided by IVD into five regions, consisting of 7 cervical vertebrae, 12 thoracic vertebrae, 5 lumbar vertebrae, 5 sacral vertebrae and 4 coccygeal vertebrae as shown in Figure 2.3 (Aleti & Motaleb, 2014). However, only the top 24 vertebrae are included in the movement of the spine in the cervical, thoracic and lumbar regions.

The cervical spine is located in the neck area with seven vertebrae numbered from C1 to C7. The lumbar spine is situated in the lower back with five vertebrae numbered by L1-L5. The role of the cervical spine is to support the head's weight while the function of the lumbar spine is to support the body's weight (Friis et al., 2017).

For thoracic spine, it is positioned in the middle back and consists of twelve vertebrae numbering from T1 to T12. It has the function of holding the rib cage and protecting the heart and lungs. The last part of the spine, which is the sacrum, is located below the lumbar spine. It consists of five fused vertebrae, which are named by S1-S5. The tail bone is normally named as the coccyx where it composed of four fused rudimentary vertebrae. The role of sacrum is to connect the spine with hip bones whereas coccyx provides attachment for ligaments and muscles of the pelvic floor.

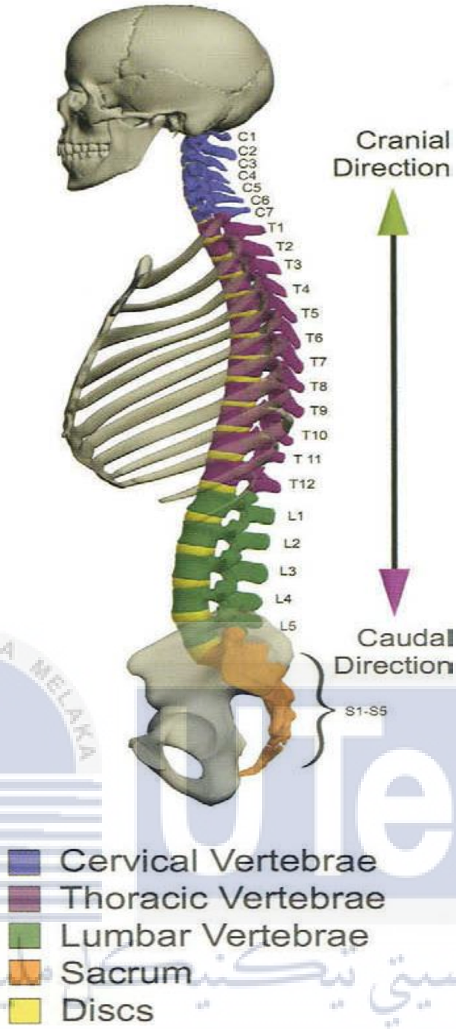

Figure 2.3: Cervical, thoracic, lumbar, and sacral regions of the spine (Kurtz & Edidin, 2006).

2.4 Human lumbar spine

Human lumbar spine is frequently activated during everyday life as its functions are to withstand the upper body weight and sustain the flexibility and stability of the body (Han et al., 2011). The vertebrae are connected to one another through articulating facet joints and IVDs as illustrated in Figure 2.4. Besides, the human lumbar spine is composed of vertebral body, posterior element, facet joints, ligaments, intervertebral discs, muscles and motion segments (Kurutz & Oroszváry, 2010).

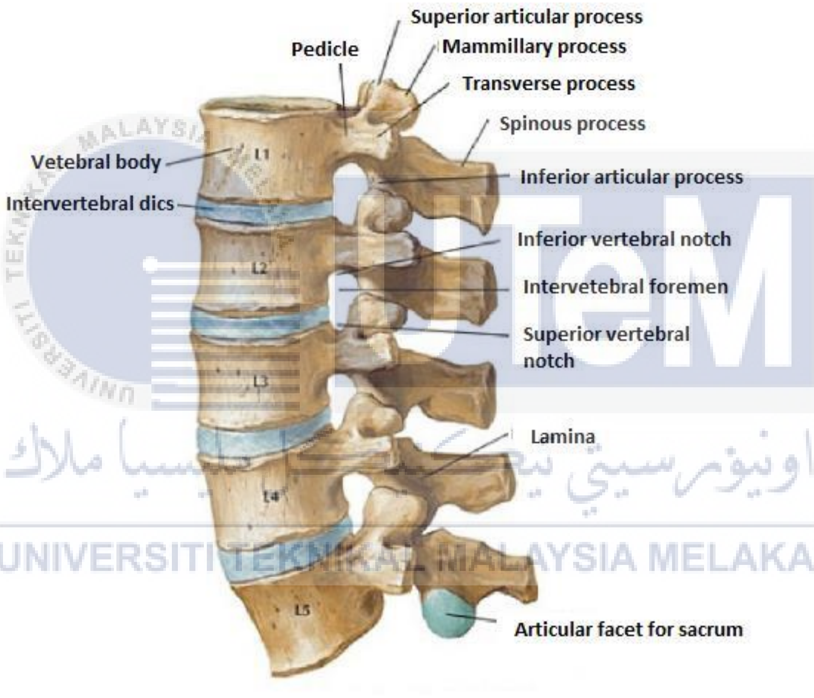

Figure 2.4: The left lateral view of the lumbar spine (Netter et al., 2006).

2.4.1 Lumbar vertebra

The three functional segments in a lumbar vertebra include vertebral body, posterior elements and pedicles that connect the vertebral body to posterior elements (Rolin & Carter, 2019). The vertebral body is the main element of the lumbar spine with a cross-section that resembles the form of a kidney (Wilke & Volkheimer, 2018). It consists of two structural components which are trabecular and cortical bone (Ritzel et al., 1997). Most posterior elements as well as the pedicles are made up of spongy bone covered by a compact bone shell.

There are a total of 5 lumbar vertebrae, with sacrum located at the end of the spine. A typical vertebra comprises of a cylindroid vertebral body and a bony arch, which also termed the neural arch, attaching to the back of the body. Between the two is the vertebral foramen (Mahadevan et al., 2018). The vertebral body lies anteriorly whereas the arch of the neural lies behind the vertebral body.

The dimensions of the vertebral body increase progressively from cephalad to caudal while the neural arch composed of a pair of pedicles, emerges from the postero-lateral surface of the upper part of the vertebral body that situated further posteriorly, which connects with paired laminae as shown in Figure 2.5 (Ebraheim et al., 2004). The vertebral bodies are comparatively large in order to withstand the high loads acting on the lumbar vertebrae, with their size increasing towards the sacrum (Wilke & Volkheimer, 2018).

Transverse process projects laterally from both side of the vertebral arch whereas spinous process projects backwards from the posterior midline of the vertebral arch. The plate-like shape in vertebral arch is termed the lamina, where it locates within the transverse and spinous processes as shown in Figure 2.6 (Mahadevan et al., 2018).

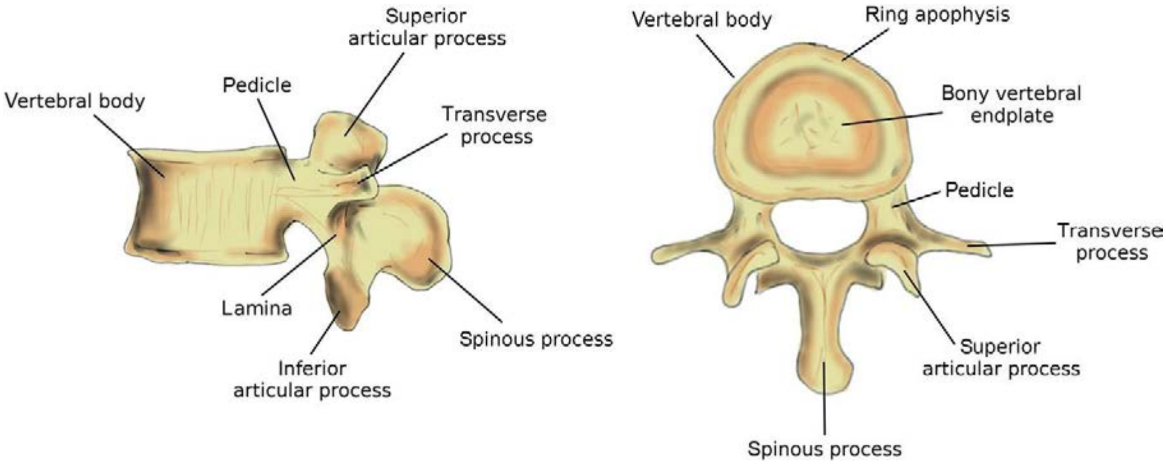

Figure 2.5: The lateral and superior views of lumbar vertebra (Wilke & Volkheimer, 2018)

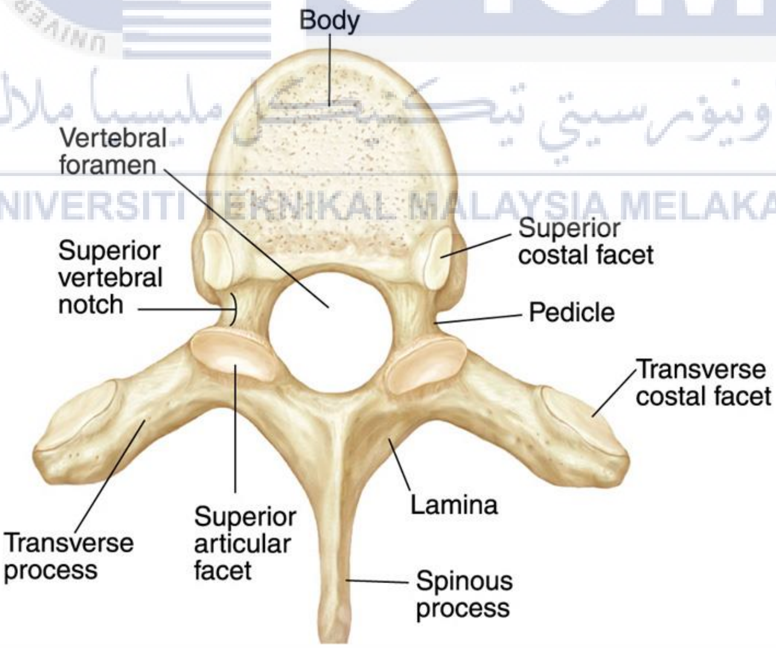

Figure 2.6: The superior view of the L2 vertebra (Mahadevan et al., 2018).

2.4.2 Intervertebral disc

Intervertebral disc (IVD) is a unique and complex structure, which lie between the vertebral bodies, are made of fibrocartilage (Newell et al., 2017). It acts as a viscoelastic cushion to allocate and reduce forces with simultaneous flexibility (Kurtz & Edidin, 2006). There are a total of 23 IVDs in a human spine, the first between C2 and C3 of the vertebral bodies while the last one at the lumbosacral junction (Mahadevan et al., 2018).

The two main regions in an IVD are the outer multi-layered fibrous ring, namely annulus fibrosus (AF) and the inner gelatinous part called nucleus pulposus (NP) (Kouroumalis et al. 2018). The layers of AF are about 0.14-0.52mm thick and the thickness increase gradually in the lateral part of the annulus (Alonso & Hart, 2014).

AF contains fibroblast-like cells while NP consists of cells resembling chondrocytes (Urban & Roberts, 2003). The AF have high tensile strength and extensibility whereas the NP acts as a hydrated gel and possesses compressibility (Mahadevan et al., 2018). Adult NP of the IVD develops into hyaline cartilage-like tissue, together with collagen II, collagen IX, and aggrecans, which is the typical signature of chondrocytes (Malandrino et al., 2018).

The characteristic of NP enables it to be distorted under pressure, but the volume of the fluid cannot be compressed. The nucleus tends to distort when subjected to pressure from any directions as shown in Figure 2.7.

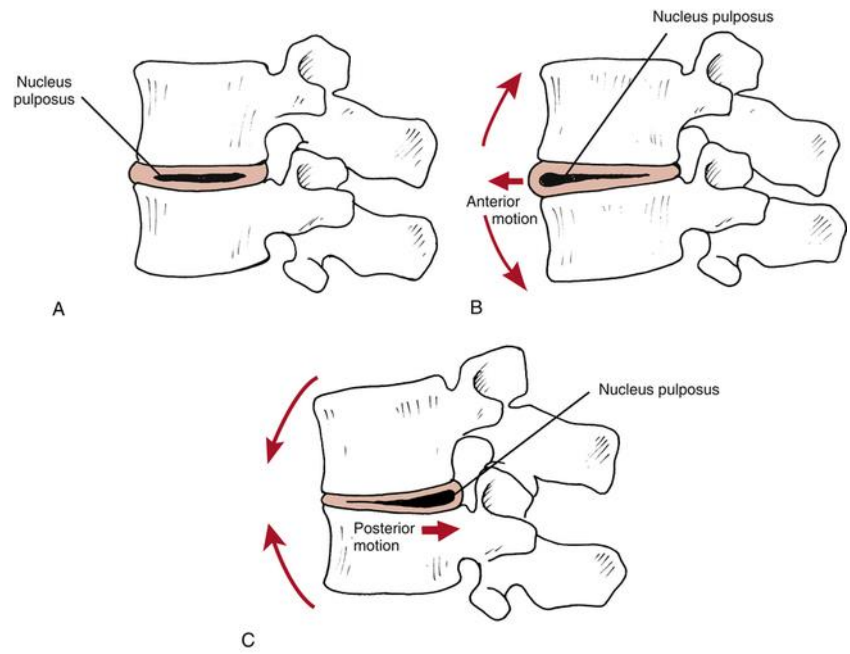

Figure 2.7: Movement of the nucleus pulposus in statis, spinal flexion to extension and extension to flexion (Sparks et al., 2017).

Vertebral endplates are another components in IVD, covering the top and bottom of the disc with two layers of cartilage as shown in Figure 2.8. It is 0.6-1mm thick for each of the endplate and both endplates cover the nucleus pulposus entirely. The adjacent vertebral bodies are separated from the disc by the vertebral endplates (Baxter et al., 2008).

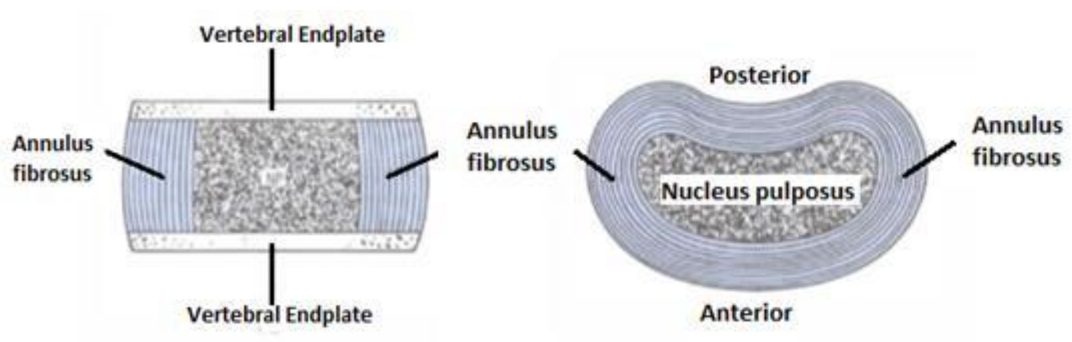

Figure 2.8: The basic structure of intervertebral disc (Baxter et al., 2008).

2.4.3 Facet joint

Facet joints or zygapophysical joints are situated on the posterior-lateral spine, act with the intervertebral disc to transmit loads experienced by the spine while enable applicable motion of the vertebrae (O'Leary et al., 2017). The facet joints composed of the adjacent inferior and superior articular processes and the articular capsule as shown in Figure 2.9. The facets of the lumbar vertebrae are ovoid, having a surface area of approximately $160 \mathrm{mm}^2$ with a height of 16mm and a width of 14mm (Baxter et al., 2008).

Hyaline cartilage, which enables the sliding movement to take place in the spinal column's back arch, encompasses the vertebral surfaces of the facet joints. The thin articular capsules are attached peripheral to the articular surfaces of the facet joints with an inner synovial and an outer fibrous membrane (Ebraheim et al., 2004). The articular cartilage of the joints can generate serious degenerative changes in which pain may occur due to the high level of mobility and the high strengths of the facet joints (Abd Latif et al., 2012).

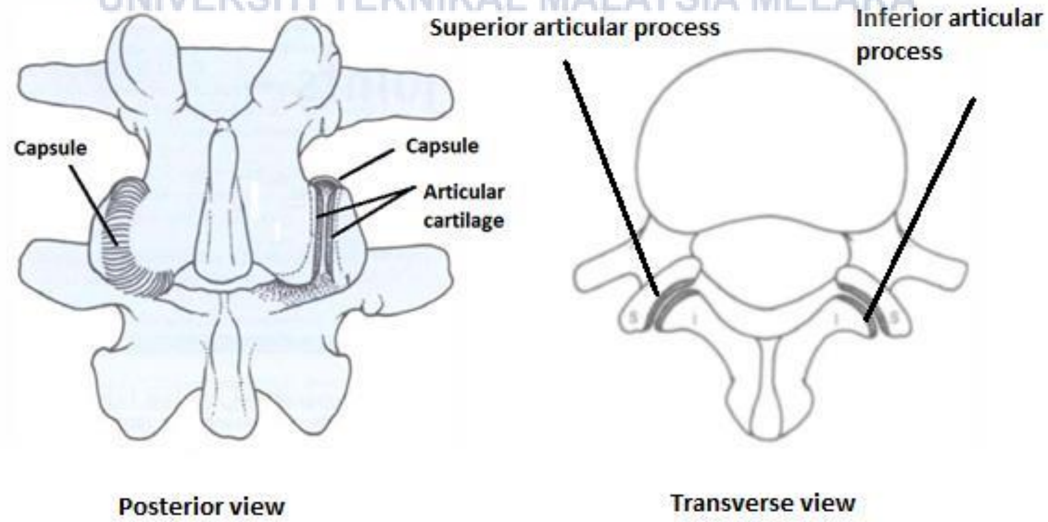

Figure 2.9: L3-L4 view of facet joint (Baxter et al., 2008).

2.4.4 Ligament

Ligaments made up of a ground substance matrix strengthened by a fibrous collagen and elastin network (Gardiner et al., 2007). The anterior longitudinal ligament with a cross-sectional area of about $32mm^2$ covers the spinal column that runs over the vertebral bodies and IVD (Rohlmann et al., 2001).

There are a total of seven ligaments attached to the lumbar spine, which are anterior longitudinal ligament (ALL), posterior longitudinal ligament (PLL), intertransverse ligament (TL), flaval ligament (LF), supraspinous ligament (SSL), facet joint capsule (CL) and interspinous ligament (ISL) as shown in Figure 2.10.

The function of the ligament is to stabilize the joints and provide a structure for the bones as it connects the bones to each other. However, due to the presence of limited stretching ability in ligaments, how far a joint moves is somehow limited in order to help protect against injury.

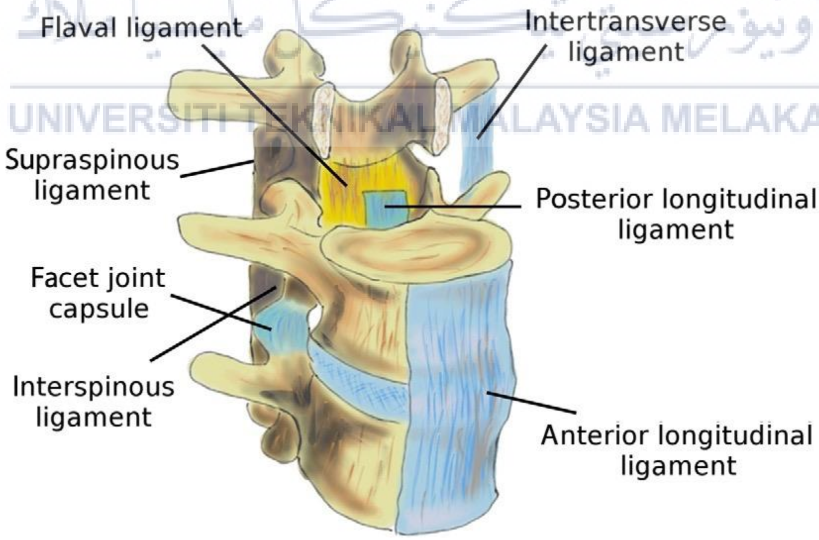

Figure 2.10: Ligaments attached to lumbar spine (Wilke & Volkheimer, 2018).

2.5 Low back pain

LBP is defined in the lumbar region of the spine as pain, muscle tension or stiffness (Violante et al., 2015). It is an illness that occurs commonly in each of the countries by people of different ages from children to the elderly person. LBP is also the number one cause of disability worldwide, characterized by psychological factors, social factors, biophysical factors, comorbidities and mechanisms for the treatment of pain (Hartvigsen et al., 2018).

2.5.1 Causes

Studies suggest that LBP may arise from potential anatomic sources such as bones, nerve roots, muscles, joints, ligaments, IVDs, blood vessels and organs in the abdomen (Allegri et al., 2016). Studies have also proven that the incidence of LBP is influenced by environmental and personal factors including low levels of education, stress, depression, anxiety, low levels of workplace social support and job dissatisfaction (Hoy et al., 2010).

Besides, among the risk factors that have been positively associated with LBP such as work activity, vibration, obesity, smoking and level of physical activity, it is suspected that obesity is the main cause of LBP where patients are frequently advised by the health care professionals to lose weight in order to reduce their symptoms (Roffey et al., 2011). A study had proven that 72% of 204 issues who received either a total hip or knee replacement were obese compared to the 26% of obese in the general community (Khoueir et al., 2009). Anatomically, the increase of the load on the lumbar spine is caused by the increase in weight. This situation will then lead to a decrease in disc hydration, changed biomechanics and deleterious stress allocation of tissues and lastly causes degeneration of disc and low back pain (Peng et al., 2018).

2.5.2 Treatments

Treatment options including spinal manipulation, yoga, acupuncture and other exercise-based therapy programs that aims for improvement in function and prevention in worsening disability are recommended specifically for LBP (Foster et al., 2018). These physical therapies focus on the strengthening of the core muscle and aerobic conditioning. However, there are a lack of conclusive scientific evidence in these therapies that support the efficacy in the treatment of LBP (Patrick et al., 2014).

Medications, namely nonsteroidal anti-inflammatory drugs (NSAIDs), acetaminophen, tramadol, muscle relaxants, opioids and antidepressants are commonly used to treat acute back pain (Patrick et al., 2014). The long-term benefits of these medications are uncertain but the side effects are well established. In order to provide long-term pain relief for LBP, the most effective techniques are the trigger point injections including dry needling, lidocaine alone or lidocaine with corticosteroid (Chen et al., 2017).

2.6 Computational studies

The finite element method (FEM), which is a mathematical technique that is widely implemented in the industry to achieve the most suitable solutions for the complicated problem by discretized a structure into several elements and described the behaviour of each element regarding the material properties, input loading and boundary condition. Since 1950s, FEM is commonly used for structural analysis in the sectors of engineering, especially in the analysis of aircraft structure and later in the field of orthopaedic biomedical research (Brekelmans et al., 1972). The use of FEM in the biomedical area including lumbar spine analysis to interpret the complex structure of living being is preferred because it not only enhances the understanding of the behavior of the spine, but also allows repeatable simulation, rapid time calculation, cost-saving and ethical concerns.

2.6.1 Material properties of human lumbar spine

The cortical bone and cancellous bone are found in anterior vertebral body where the cancellous bone is enclosed in high-density cortical bone shell. The cortical bone used in modelling is usually 1.00mm thick (Silva-Correia et al., 2013; Zhang et al., 2018). Isotropic elastic material is used frequently in previous studies in order to identify the mechanical behaviour of the bone structure in lumbar spine (Schmidt et al., 2007; Rohlmann et al., 2009; Kim et al., 2014; Zhang et al., 2018).

Since the IVD is assumed to be incompressible when load is applied to it, material law of Mooney-Rivlin is used in most studies to model hyper-elastic and incompressible behaviour of annulus fibrosus and nucleus pulposus (Schmidt et al., 2007; Park et al., 2013; Kim et al., 2014).

For the modelling of facet joint, which composed of the articular processes bone and cartilage layer, gap elements (Rohlmann et al., 2007) and spring elements (Kim et al., 2014) are used for the purpose to study the space within the two cartilage surfaces. Moreover, to simulate the synovial fluid effect at the facet joint, frictionless surface contact elements are mostly used in *in vitro* studies (Schmidt et al., 2007; Kim et al., 2014).

Besides, spring element (Schmidt et al., 2007; Rohlmann et al., 2009) and truss element (Kim et al., 2014) are widely used in the modelling of ligaments of the lumbar spine with the application of hyperelastic material properties.

The material properties for each element of human lumbar spine used in previous studies are listed according to their mechanical behaviour as shown in Table 2.1.

Table 2.1: The material properties used in modelling of lumbar spine in previous studies

Source	Cortical bone	Cancellous bone	Annulus fibrosus	Nucleus pulposus	Annulus fibers	Ligament	Cartilage of facet joint	Solver
Rohlmann et al. (2007)	E = 10000 MPa v = 0.3	E_1 = 200MPa E_2 = 140MPa v_1 = 0.45 v_2 = 0.315	Hyperelastic Neo-Hookean C_1 = 0.3448 C_2 = 0.3	Incompressible fluid-filled cavity	Non-linear dependent on distance from disc centre, 14 layers criss-cross pattern	Non-linear stress strain curve	Soft frictionless contact, Initial gap = 0.5mm	Abaqus 6.10
Schmidt et al. (2007)	E_1 = 22000MPa E_2 = 11300MPa v_1 = 0.484 v_2 = 0.203	E_1 = 200MPa E_2 = 140MPa v_1 = 0.45 v_2 = 0.315	Hyperelastic Mooney-Rivlin C_1 = 0.56 C_2 = 0.14	Incompressible fluid-filled cavity	Non-linear stress-strain curve, 16 layers criss-cross pattern	Non-linear stress strain curve	Hard frictionless contact, E = 35MPa v = 0.4 Initial gap = 0.4mm	Abaqus 6.10
Kurutz and Oroszvary (2010)	E = 12000 MPa v = 0.3	E = 150MPa v = 0.3	E = 4MPa v = 0.45 For tension, E = 0.4MPa	E = 1MPa v = 0.499 For tension, E = 0.4MPa	Tension only, E = 500MPa for external fiber, 400MPa for middle fiber and 300MPa for internal fiber	Linear elastic element, E = 8MPa for ALL E = 10MPa for PLL v = 0.35 For other ligaments, E = 5MPa v = 0.35		ANSYS Classic

Park et al. (2013)	E = 12000 MPa v = 0.3	E = 100MPa v = 0.2	Hyperelastic Mooney-Rivlin C_1 = 0.18 C_2 = 0.045	Incompressible fluid-filled cavity	Non-linear, depending on distance from center, 6 layers criss-cross parttern	Non-linear stress strain curve	Hard frictionless contact, E = 11MPa v = 0.4 Initial gap = 0.5mm	Abaqus 6.10
Kim et al. (2014)	E_1 = 22000MPa E_2 = 11300MPa v_1 = 0.484 v_2 = 0.203	E_1 = 200MPa E_2 = 140MPa v_1 = 0.45 v_2 = 0.315	Elastic E = 4.2MPa v = 0.45	Incompressible fluid-filled cavity	Non-linear stress-strain curve, 8 layers criss-cross pattern	Non-linear stress strain curve	Hard frictionless contact, E = 35MPa v = 0.4 Initial gap = 0.5mm	Abaqus 6.6
Du et al. (2016)	E = 14000 MPa v = 0.3	E = 100MPa v = 0.2	Hyperelastic Mooney-Rivlin C_1 = 0.18 C_2 = 0.045	Hyperelastic Mooney-Rivlin C_1 = 0.12 C_2 = 0.03	Calibrated stress-strain curves	Calibrated deflection-force curves	Hyperelastic Neo-Hookean C_{10} = 2	Abaqus 6.11

*E: Young's modulus; v: Poisson's ratio; C_1 and C_2: Material constant

2.7 Finite element studies for human lumbar spine

The functional spinal unit (FSU), which also known as the motion segment, can be classified into six degrees of freedom, namely 3 rotational and 3 translational (M.M. Panjabi et al., 1994; Costi et al., 2007; Kelly et al., 2013). The motions of rotational comprised of flexion-extension, axial rotation and lateral bending, while axial displacement, lateral shear and anterior shear are considered as translational motion.

2.7.1 Range of motion

Range of motion (ROM) explained the movement of the lumbar spine with regard to the angle when load is applied to it (Schulte et al., 2008; Li et al., 2009). The kinematic motion of human lumbar spine can be determined through ROM by comparing the difference in angles when carrying out activities such as flexion and extension.

2.7.2 Intradiscal pressure of nucleus pulposus

The magnitude of intradiscal pressure (IDP) of IVD is important in predicting the loading condition of the FE lumbar spine model (Kuo et al., 2010). Excessive mechanical load on the spine may result in high pressure within the nucleus pulposus and finally lead to degeneration of disc and low back pain (Urban & Roberts, 2003). The verification of the lumbar spine uses IDP of IVD to validate the reliability of FE lumbar spine model for further simulation purposes (Markolf & Morris, 1974; Ranu, 1990).

2.7.3 Stress analysis of annulus fibrosus

In order to reduce the disc height that led to severe disc degeneration in lumbar spine simulation in FE studies, the assignation of material properties of the disc is controlled (Rohlmann et al., 2001). The reduced hydrostatic pressure and disc height due to poor nutrition supply altered the load distribution where the annulus became less flexible to the applied compression, and this led to the tearing of annulus fibers (Palepu et al., 2012). Thus, it is significant to carry out stress analysis in the annulus to minimize the risk of disc degeneration.

2.7.4 Finite element model of ligaments

The geometrical component of a structure in a finite element model is segregated into small parts where each of the small portions is called an element. The points in which the elements link to each other are named as nodes. The smaller the sizing of the element, the more closely the model illustrates the actual material continuity. By using ABAQUS software, the finite element models of lumbar, thoracic and cervical spinal segments are established in three-dimensional including detailed segments such as ligaments, facet joints and IVD. The example of lumbar spine model is shown in Figure 2.11.

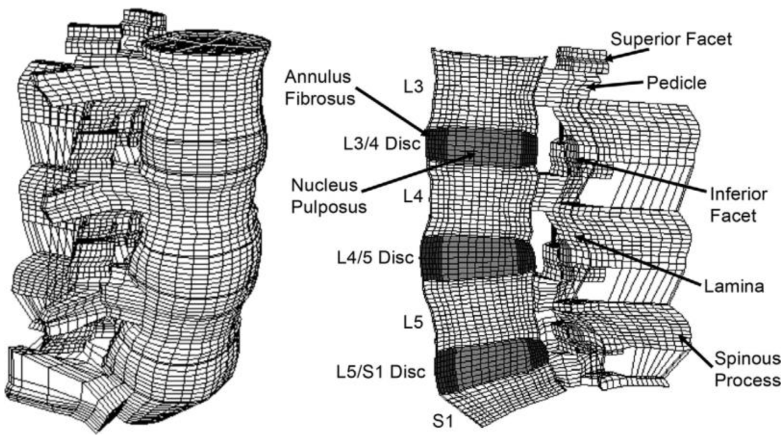

Figure 2.11: Three-dimensional finite element model of the ligamentous L3-S1 segment (Friis, 2017).

2.8 Research gap of knowledge

In general, human lumbar spine acts as the main support of upper body during daily activities. The stress of IVD in human lumbar spine increased when greater load applied on it and this situation may lead to the occurrence of LBP. Previous studies had declared that the people with overweight or obesity problem tend to suffer LBP with higher possibility (Hashimoto et al., 2017). Thus, it is vital to study the effect of various human weights on IVD by using BMI as a reference.

CHAPTER 3

METHODOLOGY

3.1 Overview

This chapter illustrates the methodology used in this project in order to develop the finite element model of human lumbar spine and ligaments. The model was then validated through verification from previous studies. The FE model was verified and then simulated by using ABAQUS software in order to analyze the biomechanical effects of IVD with various human weights. The flow chart for this study is shown in Figure 3.1.

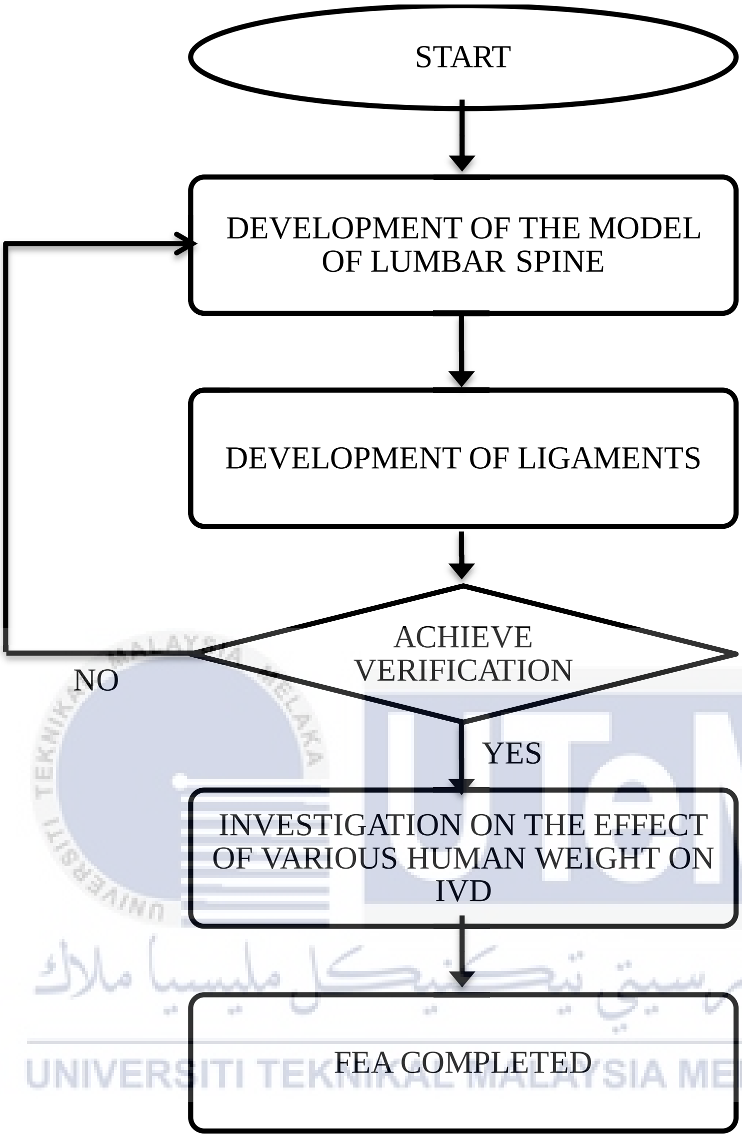

Figure 3.1: The flow chart of the methodology.

3.2 Material properties

Both cortical and cancellous bones were selected to study the linear and isotropic material properties in this study (Park et al., 2013). The facet surfaces were made smooth in order to simulate the frictionless motion between facet surfaces. By having linear elastic and isotropic material properties, the initial gap between the cartilage layers was assumed to be 0.5mm (Kim et al., 2014). Due to the hyperelastic behaviour of annulus fibrosus and fluid-like properties of nucleus pulposus, the material model of Mooney-Rivlin was used in the modelling of IVD (Schmidt et al., 2007).

To generate exact and specific biomechanical effect of lumbar spine, the material properties of FE model are assigned. The list of material properties used in the FE model of lumbar spine is shown in Table 3.1.

Table 3.1: The list of material properties used in the FE lumbar spine model

Element Set	**Material Properties**	**Reference**
Cortical bone	E = 12000MPa, v = 0.3	(Park et al., 2013)
Cancellous bone	E = 100MPa, v = 0.2	(Park et al., 2013)
Articular cartilage	E = 35MPa, v = 0.4	(Kim et al., 2014)
Nucleus pulposus	Mooney-Rivlin: $C_1 = 0.12$, $C_2 = 0.03$	(Schmidt et al., 2007)
Annulus ground substance	Mooney-Rivlin: $C_1 = 0.18$, $C_2 = 0.045$	(Schmidt et al., 2007; Park et al., 2013)

*E: Young's modulus; *v*: Poisson's ratio

3.2.1 Ligament

To model the ligaments in lumbar spine, the application of 3D truss elements were used (Kim et al., 2014). All the 7 ligaments modelled in FE lumbar spine were set as tension elements (Kurutz et al., 2005). Two types of ligament properties, namely linear behaviour and hyperelastic behaviour, were used in the modelling of ligaments in order to develop the most suitable and reliable model for analysis. The lists of material properties for linear ligaments used in FE model were illustrated in Table 3.2, while ligaments with hyperelastic behaviour were based on Ogden material model as shown in Table 3.3 (Kim et al., 2014; Chen et al., 2002). The geometric parameters of each ligament were illustrated in Table 3.4. Figure 3.2 displayed all the ligaments of lumbar spine model.

Table 3.2: Material properties of linear ligaments used in FE lumbar spine model

Ligaments	**Material Properties**	**Reference**
Anterior longitudinal ligament (ALL)	E = 20MPa, v = 0.3	(Goel et al., 1995)
Posterior longitudinal ligament (PLL)	E = 70MPa, v = 0.3	(Wang et al., 2016)
Ligamentum flavum (LF)	E = 50MPa, v = 0.3	(Chen et al., 2008)
Interspinous ligament (ISL)	E = 28MPa, v = 0.3	(Wang et al., 2016)
Supraspinous ligament (SSL)	E = 28MPa, v = 0.3	(Wang et al., 2016)
Intertransverse ligament (TL)	E = 28MPa, v = 0.3	(Wang et al., 2016)
Capsular ligament (CL)	E = 20MPa, v = 0.3	(Chen et al., 2008)

*E: Young's modulus; v: Poisson's ratio

Table 3.3: Material properties of hyperelastic ligaments used in FE lumbar spine model

Ligament	Material Properties
Anterior longitudinal ligament (ALL)	E = 7.8 MPa (ε < 12%) ; 20 MPa (ε > 12%)
Posterior longitudinal ligament (PLL)	E = 10 MPa (ε < 11%) ; 20 MPa (ε > 11%)
Ligamentum flavum (LF)	E = 15 MPa (ε < 6.2%) ; 19.5 MPa (ε > 6.2%)
Interspinous ligament (ISL)	E = 10 MPa (ε < 14%) ; 11.6 MPa (ε > 14%)
Supraspinous ligament (SSL)	E = 8 MPa (ε < 20%) ; 15 MPa (ε > 20%)
Intertransverse ligament (TL)	E = 10 MPa (ε < 18%) ; 58.7 MPa (ε > 18%)
Capsular ligament (CL)	E = 7.5 MPa (ε < 25%) ; 32.9 MPa (ε > 25%)

Table 3.4: Geometric parameters of ligaments used in FE model

Ligaments	Cross Sectional Area (mm^2)	Reference
Anterior longitudinal ligament (ALL)	63.7	(Chen et al., 2002)
Posterior longitudinal ligament (PLL)	5	(Pintar et al., 1992)
Ligamentum flavum (LF)	40	(Chen et al., 2002)
Interspinous ligament (ISL)	40	(Zhong et al., 2006)
Supraspinous ligament (SSL)	30	(Zhong et al., 2006)
Intertransverse ligament (TL)	1.8	(Goel et al., 1995)
Capsular ligament (CL)	30	(Goel et al., 1995)

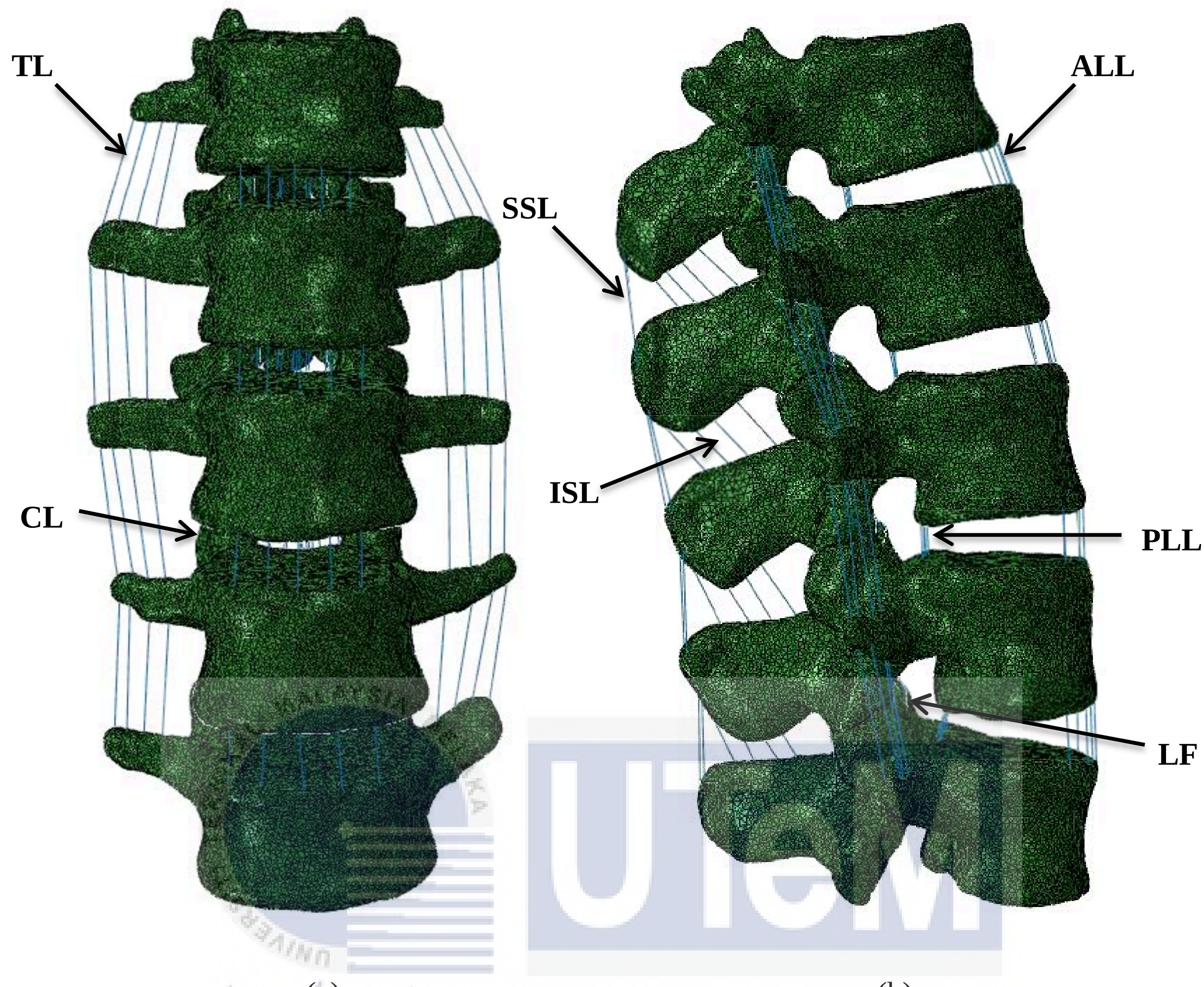

Figure 3.2: Modelling of ligaments in FE lumbar spine (a) anterior (b) lateral views.

3.3 Finite element model of lumbar spine

The FE lumbar spine model is developed using finite element software of ABAQUS 14.0 for verification and biomechanical effect purposes as shown in Figure 3.3. This lumbar spine model is obtained from the Faculty of Biosciences and Medical Engineering UTM where it is originated from a 21-year-old male volunteer with 173cm height and 70kg weight. There are a total of 1756884 tetrahedral elements and 355028 nodes in the model of the lumbar spine.

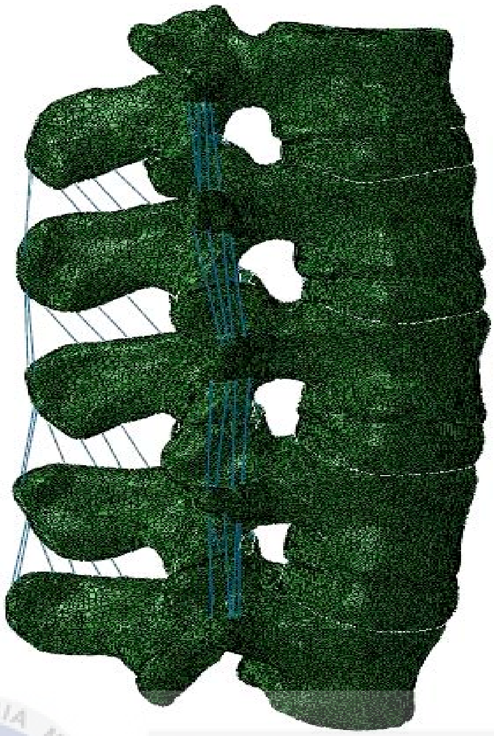

Figure 3.3: FE model of lumbar spine with ligaments modelling.

3.4 Loading and boundary conditions

The FE model of the 3-D lumbar spine was compared with previous *in vitro* study under pure moments of 7.5 Nm for two types of motions, which are flexion and extension (Manohar M. Panjabi et al., 1993). The purpose of this verification is to ensure the stability of the FE model. The force couple for flexion and extension were calculated and presented in Table 3.5. The inferior surface of L5 vertebral body was fixed as shown in Figure 3.4. The value of force couple was calculated by using the equation of moment as shown in the equation (3.1).

$$M = F_R \times d \qquad (3.1)$$

Where M is the moment, F_R is the resultant force and d is the distance between anterior and posterior of the vertebral body.

The equation of moment was rearranged to determine F_y and F_Z as shown below:

$$F_R = \frac{7.5\ Nm}{0.03m}$$

$$F_R = 250\ \text{N}$$

$$\text{Since } F_R = \sqrt{{F_y}^2 + {F_z}^2}$$

Let $F_y = 0.3\ F_s$ (30% of force acting on y-axis);

$F_z = 0.7\ F_s$ (70% of force acting on z-axis)

Therefore;

$$250\ \text{N} = \sqrt{(0.3F_s)^2 + (0.7F_s)^2}$$

$$F_s = 328\ \text{N}$$

Hence;

$$F_y = 0.3\ F_s = 0.3 \times 328\ \text{N} = 98\ \text{N}$$

$$F_z = 0.7\ F_s = 0.7 \times 328\ \text{N} = 230\ \text{N}$$

Table 3.5: Magnitude of force in y and z direction on the FE model

Loading Direction	**Anterior Point**		**Posterior Point**	
	F_y **(N)**	F_Z **(N)**	F_y **(N)**	F_Z **(N)**
Flexion	-98	-230	98	230
Extension	98	230	-98	-230

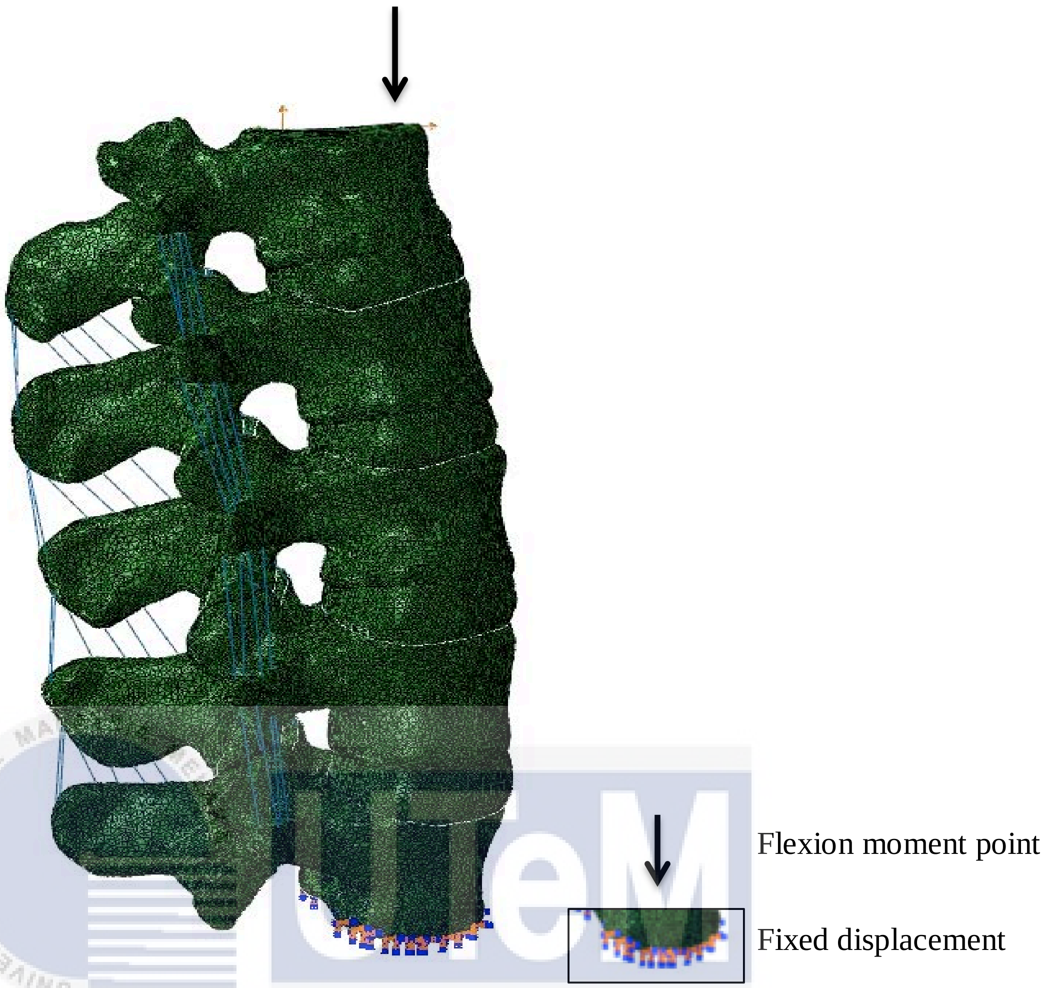

Figure 3.4: The loading and boundary conditions of FE L1-L5 lumbar spine model.

3.5 Verification of finite element model

Verification and validation of the computational study models are the essential requirements in order to develop a reliable FE model in the field of biomechanics. This step is important as an unverified or invalidated model can lead to false conclusions (Henninger et al., 2010). A verification study on the intersegmental rotations of the lumbar spine and the IVD stresses were performed in this study to verify the 3-D lumbar spine FE model. This verification must be succeeded before further simulations of biomechanical effect of lumbar spine in various human weights are investigated.

3.5.1 Intersegmental rotations of lumbar spine

To verify the stability of the FE spine model, intersegmental rotations were calculated. The comparison between L1-L5 FE lumbar spine model and previous *in vitro* study was done by using pure moments of 7.5 Nm for flexion and extension motions (M.M. Panjabi et al., 1994). The intersegmental rotations are important elements in FE modelling in order to ensure the reliability of the model.

3.5.2 Compression of intervertebral disc

The verification of IVD was performed by comparing the IDP and axial displacement to the previous *in vitro* studies (Markolf & Morris, 1974). A vertical compressive load of 1200N was applied to the L4 superior vertebral body as pressure distribution while the inferior surface of L5 vertebral body was set as fixed displacement by limiting the rotation and translation. The loading and boundary condition of FE model for range of motion (ROM) verification in ABAQUS was shown in Figure 3.5.

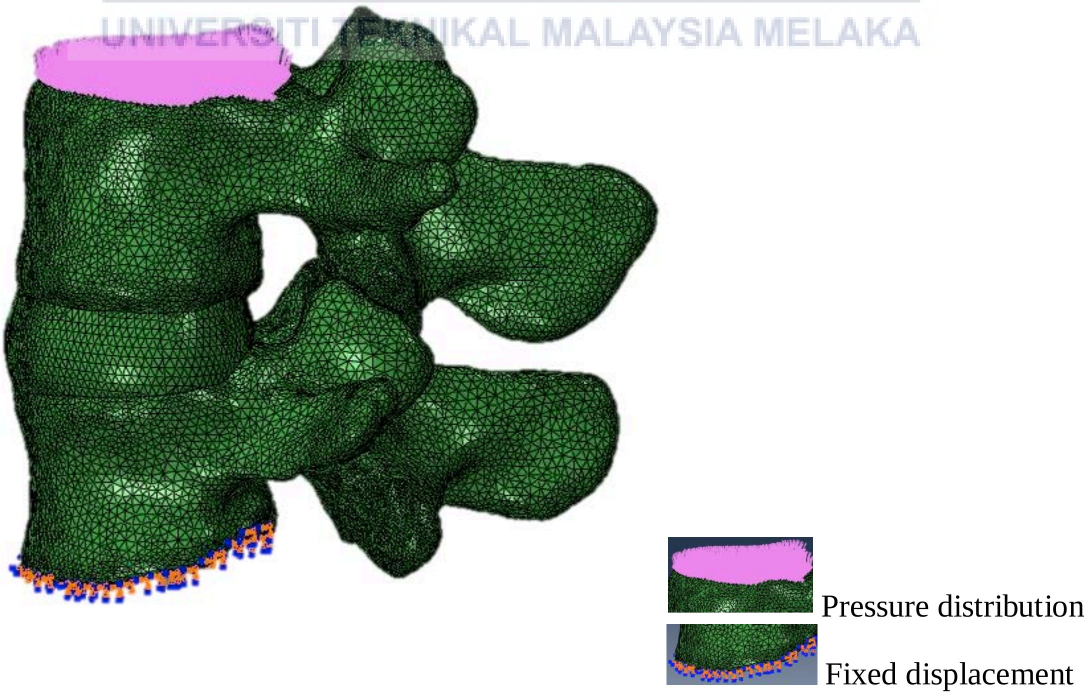

Figure 3.5: The loading and boundary condition of L4-L5 FE lumbar spine model.

3.6 Finite element analysis of lumbar spine model at various human weights

The application of 7.5 Nm pure moments and compressive follower load were done to imitate the concept of flexion and extension in lumbar spine model. The follower load method by using previous *in vitro* study was used in order to apply compressive follower load (Patwardhan et al., 1999). In order to prevent FE model from producing unnecessary moments and allowing the application of greater load on the model, follower load was implemented according to the curvature of the human spine. The stabilization of the spine can be achieved because it showed identical effect to local muscles (Rohlmann et al., 2001).

The compressive load acted on the FE lumbar spine model illustrated the upper body weight of human. About 58-60% of human body weight with an addition of muscle force is generally the weight of the upper body (Kurutz & Oroszváry, 2010). According to BMI, the weights for normal, overweight and obese at the height of 1.73m were 55kg, 80kg and 110kg, respectively. Thus, the compressive load of 700N, 900N and 1300N were simulated to study the biomechanical effect of the lumbar spine.

CHAPTER 4

RESULTS AND DISCUSSION

4.1 Overview

This chapter reports and discusses the results obtained from the lumbar spine model simulation. The L1-L5 FE lumbar spine model was verified based on the range of motion, intradiscal pressure and axial displacement of intervertebral disc. The biomechanical effects of various human weights on the finite element model during flexion and extension were studied.

4.2 The effects of ligaments in FE model of lumbar spine

One or more membrane elements are modeled for each ligament due to the bending can be ignored as ligaments are very thin structures (Eberlein et al., 2004). According to previous *in vitro* study, different ligament property will result in observable variations (Naserkhaki et al., 2018).

4.2.1 Intersegmental rotation of lumbar spine model

The FE lumbar spine model of L1-L5 was verified by the comparison of ROM under flexion at pure moment of 7.5Nm (M.M. Panjabi et al., 1994). In overall, the results of model with and without ligament showed similar curve trend with previous *in vitro* study as shown in Figure 4.1. The percentage difference of ROM under flexion at 7.5 Nm for model without ligament reached 35.65% while the percentage difference for model with ligament was 19.75%. From the results obtained, it can conclude that further improvement is needed in order to obtain reliable results from the FE model.

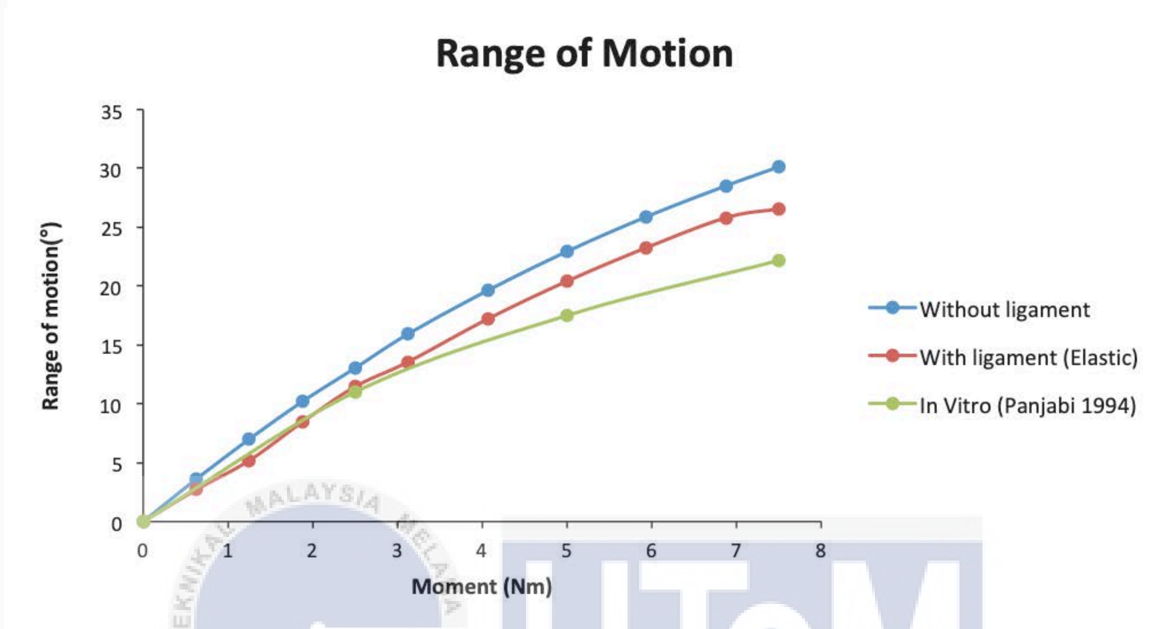

Figure 4.1: The comparison of ROM of the lumbar spine under pure moments of 7.5 Nm between present FE lumbar spine model (without ligament and with elastic ligament) and previous *in vitro* study (Panjabi et al., 1994).

4.2.2 Intervertebral disc

In flexion, different model of L4-L5 lumbar spine showed different IDP values having identical trends (Naserkhaki et al., 2018). Ligaments with elastic properties were modeled to verify the reliability of the FE model. As seen from Figure 4.2, the difference for axial displacement at 1200N compression load for FE model with and without elastic ligament when compared to previous *in vitro* study were 40.2% and 59.7% respectively. The percentage difference of IDP between present FE model with elastic ligament and FE model without ligament revealed 63.9% and 29.2% respectively compared to previous *in vitro* studies (Markolf & Morris, 1974). Based on these results, the developed FE model with elastic ligament modelling was with limited validity and could not produce appropriate and reliable results in FE analysis.

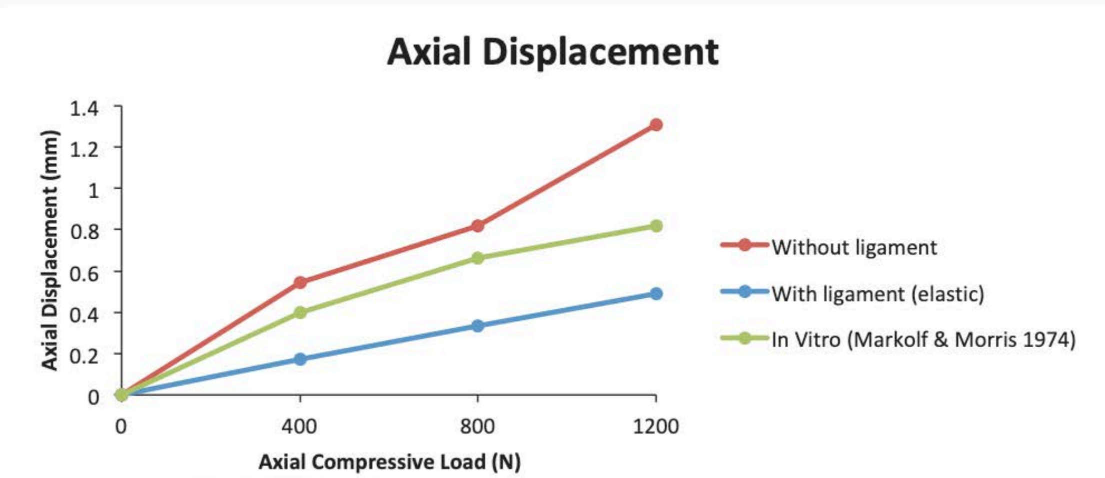

(a)

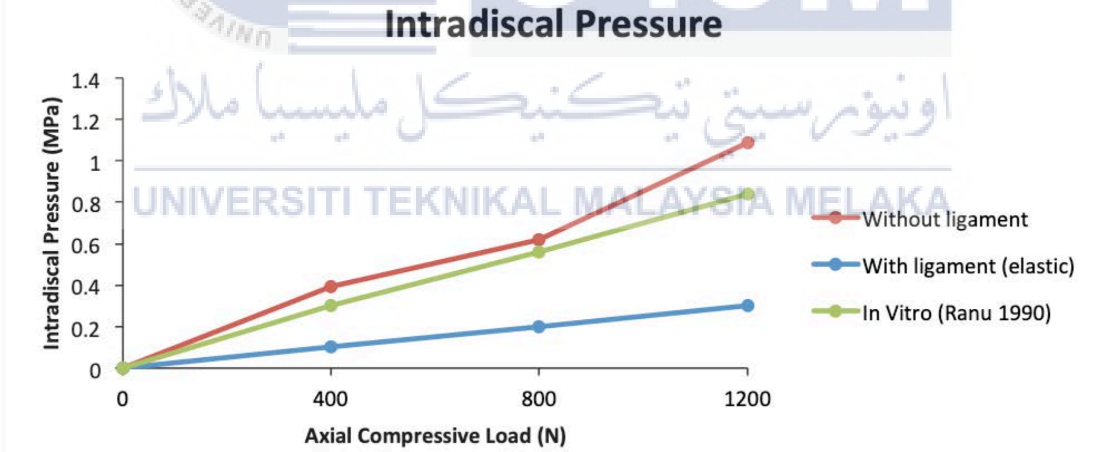

(b)

Figure 4.2: Comparison of present FE lumbar spine model (without ligament and with elastic ligament) with previous *in vitro* studies of the IVD results (a) Axial displacement (b) Intradiscal pressure under compressive load up to 1200N.

4.3 Verification of hyperelastic ligaments

The FE model of L1-L5 lumbar spine was verified by comparing the ROM with *in vitro* study for flexion at pure moment of 7.5 Nm (Panjabi et al., 1994). The deformation of lumbar spine under flexion motion is shown in Figure 4.3. The percentage difference of the ROM in flexion reached 8.33% at 1.8Nm. Since the value of ROM in this FEA study was still within the accepted range reported in the literature, the FE model could imitate the real lumbar spine's flexion motion.

IVD was verified by comparing the axial displacement and IDP of FE spine model with hyperelastic ligaments modelling in this study with previous *in vitro* studies as shown in Figure 4.4 and Figure 4.5 (Markolf & Morris, 1974; Ranu, 1990). The percentage difference of axial displacement and IDP of the IVD with previous *in vitro* studies revealed 10.2% and 9.1% respectively under compressive load of 1200N. Both axial displacement and IDP values showed a growing linear stress pattern when applied to greater loads in experiment (Faria et al., 2015). These results show that the FE model in this study could produce reliable results for the FE analysis.

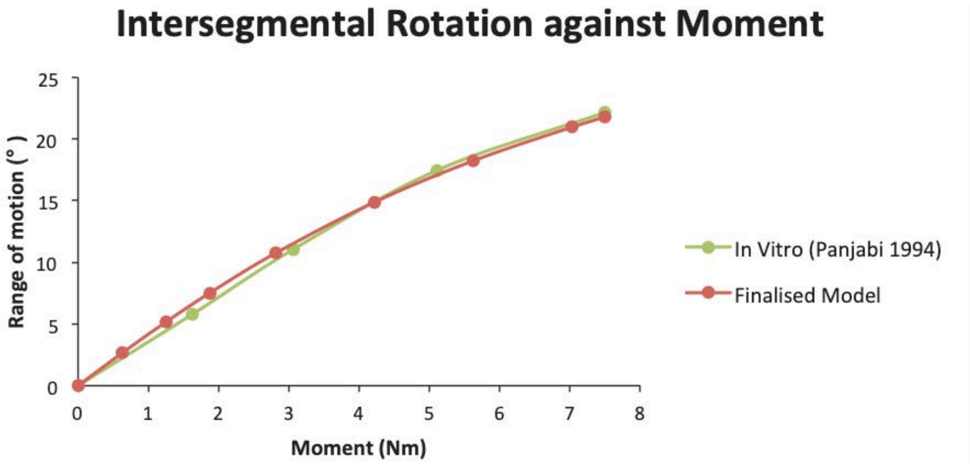

Figure 4.3: The comparison of ROM for L1-L5 lumbar spine under pure moments up to 7.5 Nm between present FE model and previously published *in vitro* result (M.M. Panjabi et al., 1994)

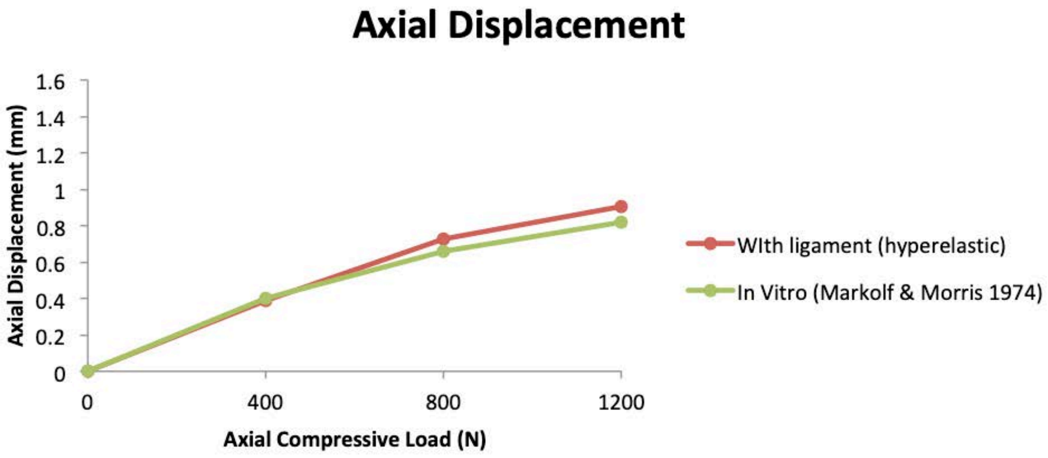

Figure 4.4: Comparison of present axial displacement of FE lumbar spine model (with hyperelastic ligament) with previous *in vitro* study (Markolf & Morris, 1974).

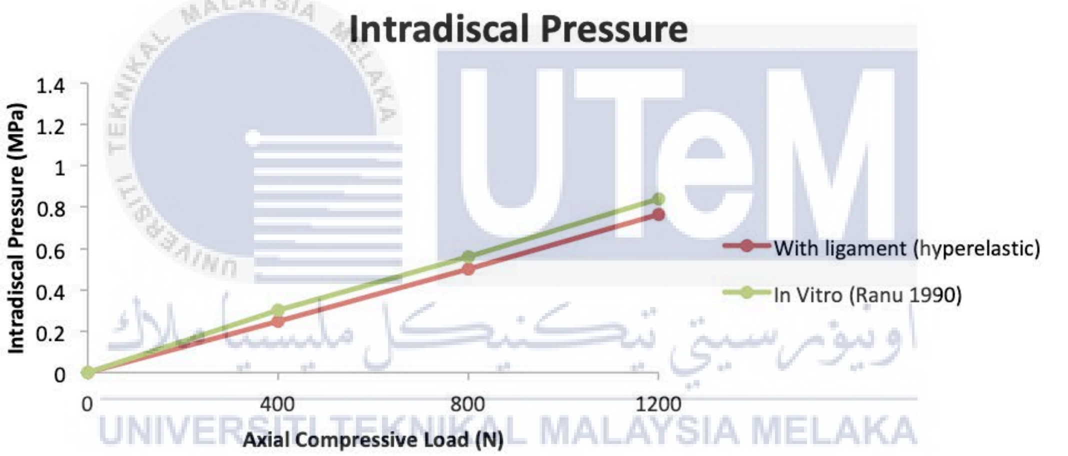

Figure 4.5: Comparison of present intradiscal pressure of FE lumbar spine model (with hyperelastic ligament) with previous *in vitro* study (Ranu, 1990).

4.4 The effects of human weight on kinematics of lumbar spine

The biomechanical effects of normal, overweight and obese on the kinematics of the lumbar spine and the stresses of the IVD were analyzed by using the verified FE lumbar spine model. The biomechanical effect of IVD can be classified into two categories, which are IDP in nucleus pulposus and VMS in annulus fibrosus.

4.4.1 The effects of human weight on intradiscal pressure of nucleus pulposus

The comparisons of intradiscal pressure in nucleus pulposus between normal, overweight and obese under flexion motion are illustrated in Figure 4.6 while the stress distribution in nucleus pulposus under flexion is as shown in Figure 4.7. The highest IDP of nucleus pulposus occurred in L4-L5 segment under combination of obese compressive load of 1300N with 1.83MPa while the segment of L3-L4 showed the lowest IDP of nucleus pulposus with 0.65MPa under flexion motion. It was found that the IDP increased with greater loads on the human spine at all levels of the IVD in flexion motion. Due to the load shift from posterior to anterior of the IVD, maximum IDP was observed to be in flexion motion. The results of the present study showed a similar trend with *in vitro* study, where the effects of human weight were noticed to be more severe particularly at L4-L5 segment in flexion motion for heavier individuals (Zahari et al., 2017). Degenerative changes were negligible in L3-L4 segment which resulted in lowest IDP of nucleus pulposus (Code et al., 2003).

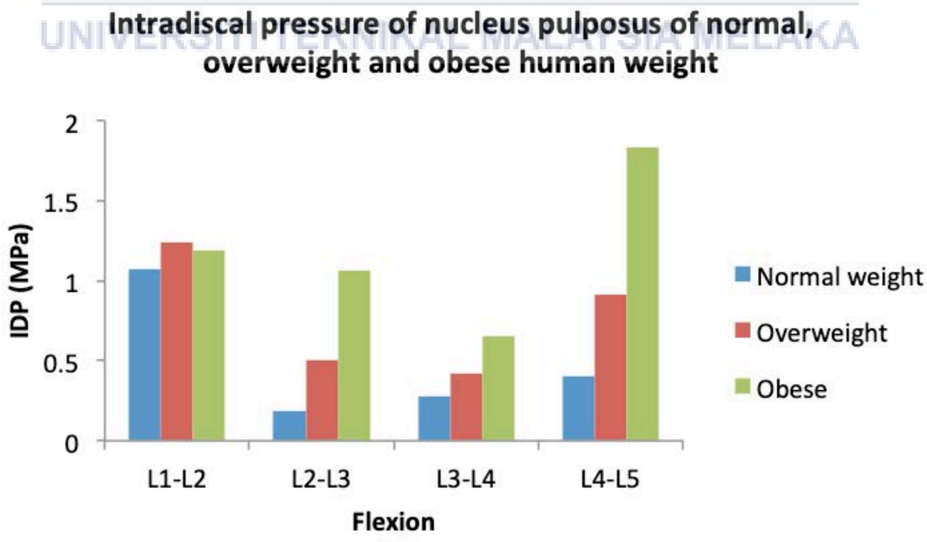

Figure 4.6: The intradiscal pressure of nucleus pulposus of normal, overweight and obese under flexion motion.

	700N	900N	1300N
L1-L2	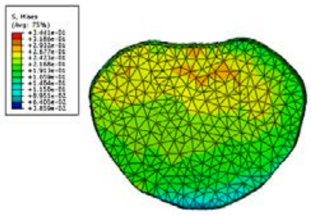	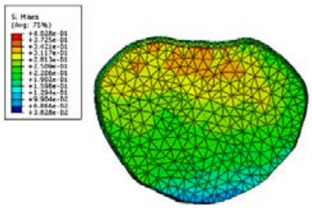	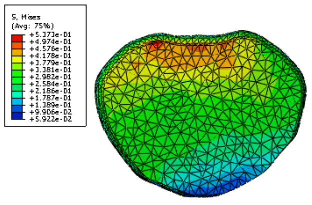
L2-L3	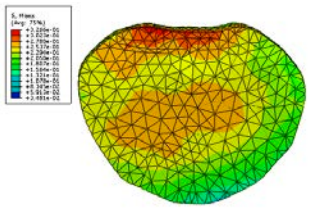	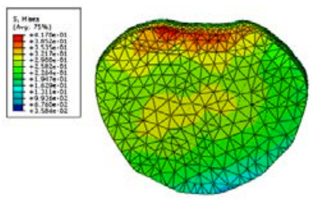	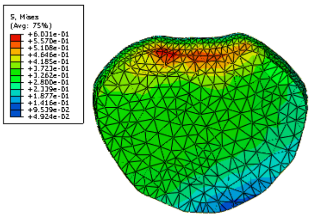
L3-L4	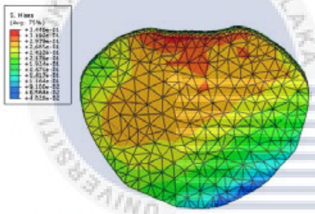	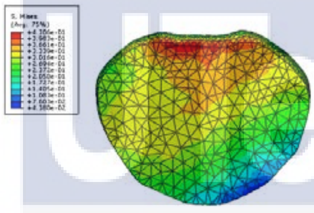	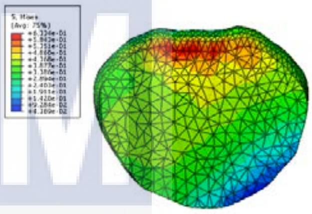
L4-L5	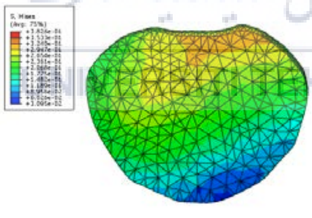	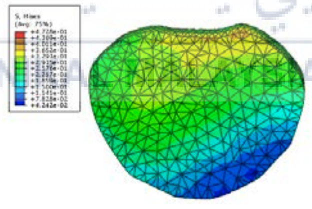	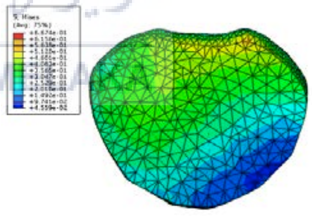

Figure 4.7: The stress distribution in the nucleus pulposus of normal, overweight and obese under flexion motion.

4.4.2 The effects of human weight on von mises stress of annulus fibrosus

A study had stated that the highest compressive stress was observed to be in the annulus fibrosus of IVD in human lumbar spine (Adams et al., 2003). In most cases, the VMS increased with the increment of human weight and reached the maximum annulus stress of 2.15MPa for 1300N at L1-L2 lumbar segment under flexion motion as shown in Figure 4.8.

The biggest difference of VMS between normal, overweight and obese under flexion motion was observed at L4-L5 segment, which followed the similar trend with previous in vitro study (Zahari et al., 2017). During flexion motion for L4-L5 segment, overweight and obese loads resulted in 13.3% and 58.3% higher than normal weight loading condition, respectively. For segments other than L4-L5, the differences in the VMS under flexion motion were 12.7-15.6% and 36.9-50%, respectively. The stress distributions in annulus fibrosus under flexion for normal, overweight and obese were illustrated in Figure 4.9.

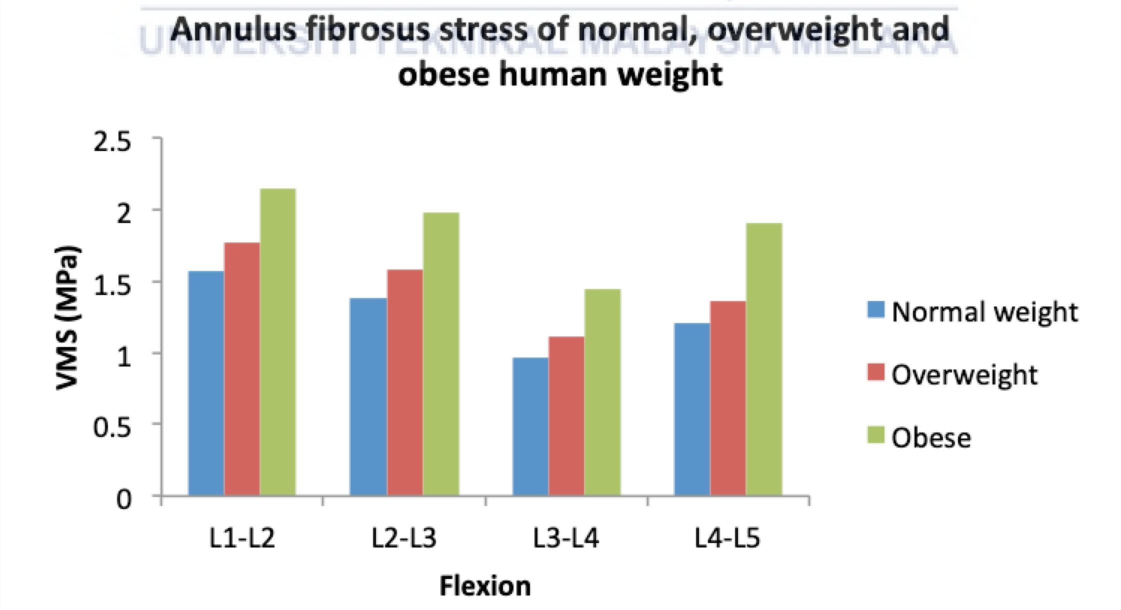

Figure 4.8: The annulus fibrosus stress of normal, overweight and obese under flexion motion.

	700N	900N	1300N
L1-L2	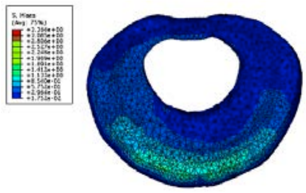	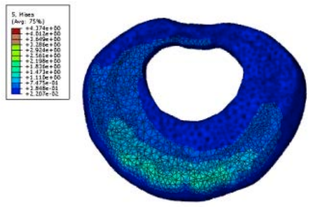	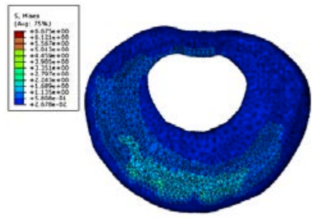
L2-L3	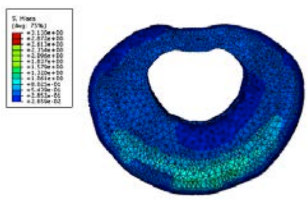	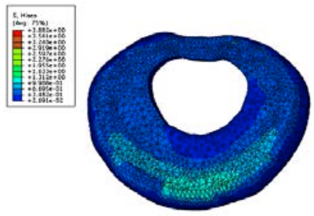	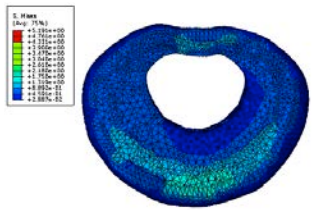
L3-L4	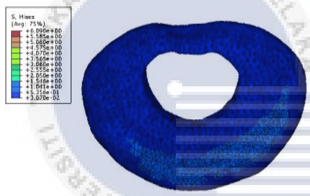	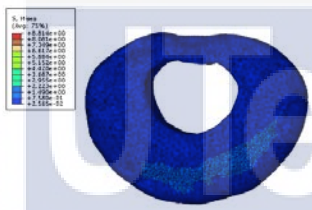	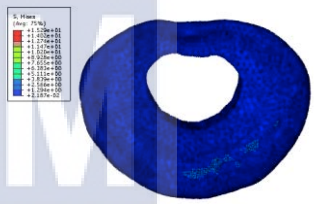
L4-L5	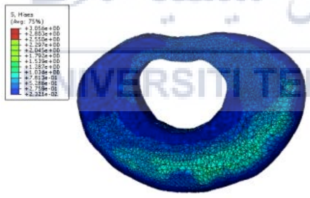	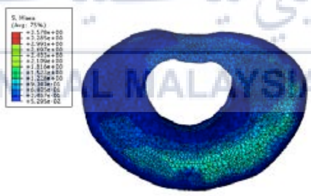	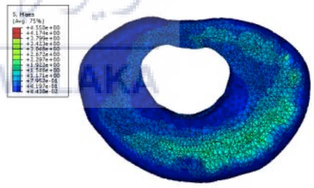

Figure 4.9: The stress distribution in the annulus fibrosus of normal, overweight and obese under flexion motion.

CHAPTER 5

CONCLUSION AND RECOMMENDATION FOR FUTURE RESEARCH

5.1 Conclusion

The purpose of this study is to investigate the biomechanical effect of IVD by using FE model under various human weights. The FE model of human lumbar spine can be used for repeated simulation, which is cost-efficient, time saving and ethical concern. A verified FE lumbar spine model can produce reliable and accurate result in lumbar spine model in terms of kinematic motion, stress distribution and intradiscal pressure.

Generally, the increase of human weight had proved to affect the kinematics of human lumbar spine, as it will increase the IVD stresses, specifically at the nucleus pulposus and annulus fibrosus. Individuals with greater body weight will tend to experience an increase in stresses of IVD in spine, and these can increase the risk of disc degeneration in which may lead to the occurrence of LBP.

5.2 Recommendations for future research

Several assumptions regarding the modelling and analysis of the lumbar spine under various loadings were taken into consideration. Throughout the study, computational methodology was used for the purpose of analysis. The present study is a non-biological experiment, in which factors such as ageing and anatomical variances were not included in the analysis. Other than that, the present study had not considered soft tissue, muscle and fat in the analysis. These restrictions may affect the results obtained and prevent the simulations of the real clinical scenario.

It is suggested that this study could be carried on by the application of three-dimensional model of ligaments to study the mechanical behaviour of spine under different loadings. Other aspects such as the effects of human weight on IVD under different motions such as lateral bending and axial torsion should be considered in future studies.

REFERENCES

Abd Latif, M. J., Jin, Z., & Wilcox, R. K. (2012). Biomechanical characterisation of ovine spinal facet joint cartilage. *Journal of Biomechanics*, *45*(8), 1346–1352.

Abi-Hanna, D., Kerferd, J., Phan, K., Rao, P., & Mobbs, R. (2018). Lumbar Disk Arthroplasty for Degenerative Disk Disease: Literature Review. *World Neurosurgery*, *109*, 188–196.

Adams, M. A., McNally, D. S., & Dolan, P. (2003). "Stress" distributions inside intervertebral discs. *The Journal of Bone and Joint Surgery*, *78*(6), 965–972.

Aleti, H., & Motaleb, I. A. (2014). Study of stress and strain in human spine. *IEEE International Conference on Electro Information Technology*, 184–189.

Allegri, M., Montella, S., Salici, F., Valente, A., Marchesini, M., Compagnone, C., … Fanelli, G. (2016). Mechanisms of low back pain: a guide for diagnosis and therapy. *F1000Research*, *5*, 1530.

Alonso, F., & Hart, D. J. (2014). Intervertebral Disk. *Encyclopedia of the Neurological Sciences*, *2*, 724–729.

Bashkuev, M., Reitmaier, S., & Schmidt, H. (2018). Effect of disc degeneration on the mechanical behavior of the human lumbar spine: a probabilistic finite element study. *The Spine Journal*.

Baxter, R., Hastings, N., Law, A., & Glass, E. J. . (2008). Clinical Anatomy of the Lumbar Spine and Sacrum. *Animal Genetics*, *39*(5), 561–563.

Bongert, C., Jansen, J., & Kreutz, E. (2004). Kommunikation, Gruppenprozesse, Mediation, Moderation. *Gruppendynamik Zeitschrift Für Angewandte Sozialpsychologie*, *77*(September 2010), 55–77.

Brekelmans, W. A. M., Poort, H. W., & Slooff, T. J. J. H. (1972). A new method to analyse the mechanical behaviour of skeletal parts. *Acta Orthopaedica*, *43*(5), 301–317.

Chen, C.-S., Cheng, C.-K., Liu, C.-L., & Lo, W.-H. (2002). Stress analysis of the disc adjacent to interbody fusion in lumbar spine. *Medical Engineering & Physics*, *23*(7), 485–493.

Chen, K. Y., Shaparin, N., & Gritsenko, K. (2017). *Low back pain*. *Pain Medicine: An Essential Review*. Elsevier Inc.

Chen, S. H., Tai, C. L., Lin, C. Y., Hsieh, P. H., & Chen, W. P. (2008). Biomechanical comparison of a new stand-alone anterior lumbar interbody fusion cage with established fixation techniques - A three-dimensional finite element analysis. *BMC Musculoskeletal Disorders*, *9*, 1–10.

Clarencon, F., Law-Ye, B., Bienvenot, P., Cormier, É., & Chiras, J. (2016). The Degenerative Spine. *Magnetic Resonance Imaging Clinics of North America*, *24*(3), 495–513.

Code, U. S., Steffen, T., Baramki, H. G., Rubin, R., Antoniou, J., & Aebi, M. (2003). U Of W HSB LIBARY Lumbar intradiscal pressure measured in the anterior and posterolateral annular regions during asymmetrical loading, *98*(3), 495–505.

Costi, J. J., Stokes, I. A., Gardner-Morse, M., Laible, J. P., Scoffone, H. M., & Iatridis, J. C. (2007). Direct measurement of intervertebral disc maximum shear strain in six degrees of freedom: Motions that place disc tissue at risk of injury. *Journal of Biomechanics*, *40*(11), 2457–2466.

Eberlein, R., Holzapfel, G. A., & Fröhlich, M. (2004). Multi-segment FEA of the human lumbar spine including the heterogeneity of the annulus fibrosus. *Computational Mechanics*, *34*(2), 147–163.

Ebraheim, N. A., Hassan, A., Lee, M., & Xu, R. (2004). Functional anatomy of the lumbar spine. *Seminars in Pain Medicine*, *2*(3), 131–137.

Faria, S. P. (2015). Biomechanical Analysis of the Human Lumbar Spine An Experimental and Computational Approach.

Foster, N. E., Anema, J. R., Cherkin, D., Chou, R., Cohen, S. P., Gross, D. P., … Woolf, A. (2018). Prevention and treatment of low back pain: evidence, challenges, and promising directions. *The Lancet*, *391*(10137), 2368–2383.

Friis, E. A., Arnold, P. M., & Goel, V. K. (2017). *Mechanical testing of cervical, thoracolumbar, and lumbar spine implants*. *Mechanical Testing of Orthopaedic Implants*. Elsevier Ltd.

Gardiner, J. C. (2007). Computational Modeling of Ligament Mechanics. *Development*, *134*(4), 635–646.

Goel, V. K. (1995). Interlaminar Shear Stresses and Laminae Separation in a Disc.

Granata, K. P., Slota, G. P., & Wilson, S. E. (2004). Influence of Fatigue in Neuromuscular Control of Spinal Stability. *Human Factors: The Journal of the Human Factors and Ergonomics Society*, *46*(1), 81–91.

Guidi, E. (1994). Anatomy and examination of the elbow. *Journal of Back and Musculoskeletal Rehabilitation*, *4*(1), 7–16.

Han, K. S., Rohlmann, A., Yang, S. J., Kim, B. S., & Lim, T. H. (2011). Spinal muscles can create compressive follower loads in the lumbar spine in a neutral standing posture. *Medical Engineering and Physics*, *33*(4), 472–478.

Hartvigsen, J., Hancock, M. J., Kongsted, A., Louw, Q., Ferreira, M. L., Genevay, S., … Woolf, A. (2018). What low back pain is and why we need to pay attention. *The Lancet*, *391*(10137), 2356–2367.

Hashimoto, Y., Matsudaira, K., Sawada, S. S., Gando, Y., Kawakami, R., Kinugawa, C., … Naito, H. (2017). Obesity and low back pain: a retrospective cohort study of Japanese males. *Journal of Physical Therapy Science*, *29*(6), 978–983.

Henninger, H. B., Reese, S. P., Anderson, A. E., & Weiss, J. A. (2010). Validation of computational models in biomechanics. *Proceedings of the Institution of Mechanical Engineers, Part H: Journal of Engineering in Medicine*, *224*(7), 801–812.

Hortin, M. (2015). Ligament model fidelity in finite element analysis of the human lumbar spine. *Mechanical Engineering*, *MS*.

Hoy, D., Brooks, P., Blyth, F., & Buchbinder, R. (2010). The Epidemiology of low back pain. *Best Practice and Research: Clinical Rheumatology*, *24*(6), 769–781.

Izzo, R., Guarnieri, G., Guglielmi, G., & Muto, M. (2013). Biomechanics of the spine. Part I: Spinal stability. *European Journal of Radiology*, *82*(1), 118–126.

Karppinen, J., Shen, F. H., Luk, K. D. K., Andersson, G. B. J., Cheung, K. M. C., & Samartzis, D. (2011). Management of Degenerative Disk Disease and Chronic Low Back Pain. *Orthopedic Clinics of North America*, *42*(4), 513–528.

Kelly, B. P., & Bennett, C. R. (2013). Design and validation of a novel Cartesian biomechanical testing system with coordinated 6DOF real-time load control: Application to the lumbar spine (L1-S, L4-L5). *Journal of Biomechanics*, *46*(11), 1948–1954.

Khoueir, P., Black, M. H., Crookes, P. F., Kaufman, H. S., Katkhouda, N., & Wang, M. Y. (2009). Prospective assessment of axial back pain symptoms before and after bariatric weight reduction surgery. *Spine Journal*, *9*(6), 454–463.

Kim, H. J., Kang, K. T., Chang, B. S., Lee, C. K., Kim, J. W., & Yeom, J. S. (2014). Biomechanical analysis of fusion segment rigidity upon stress at both the fusion and adjacent segments -A comparison between unilateral and bilateral pedicle screw fixation-. *Yonsei Medical Journal*, *55*(5), 1386–1394.

Kouroumalis, A., Mavrogonatou, E., Savvidou, O. D., Papagelopoulos, P. J., Pratsinis, H., & Kletsas, D. (2018). Major traits of the senescent phenotype of nucleus pulposus intervertebral disc cells persist under the specific microenvironmental conditions of the tissue. *Mechanisms of Ageing and Development*, (May), 0–1.

Kuo, C. S., Hu, H. T., Lin, R. M., Huang, K. Y., Lin, P. C., Zhong, Z. C., & Hseih, M. L. (2010). Biomechanical analysis of the lumbar spine on facet joint force and intradiscal pressure - A finite element study. *BMC Musculoskeletal Disorders*, *11*, 5–8.

Kurtz, S. M., & Edidin, A. A. (2006). The Basic Tools and Terminology of Spine Treatment. *Spine Technology Handbook*, 1–9.

Kurutz, M. (2005). Finite Element Modeling of the Human Lumbar Spine, (1987).

Kurutz, M., & Oroszváry, L. (2010). Finite element analysis of weightbath hydrotraction treatment of degenerated lumbar spine segments in elastic phase. *Journal of Biomechanics*, *43*(3), 433–441.

Lake, J. K., Power, C., & Cole, T. J. (2000). Back pain and obesity in the 1958 British birth cohortcause or effect? *Journal of Clinical Epidemiology*, *53*(3), 245–250.

Li, G., Wang, S., Passias, P., Xia, Q., Li, G., & Wood, K. (2009). Segmental in vivo vertebral motion during functional human lumbar spine activities. *European Spine Journal*, *18*(7), 1013–1021.

Mahadevan, V. (2018). Anatomy of the vertebral column. *Surgery (United Kingdom)*, *36*(7), 327–332.

Malandrino, A. (2018). Intervertebral Disc.

Manchikanti, L., Singh, V., Falco, F. J. E., Benyamin, R. M., & Hirsch, J. A. (2014). Epidemiology of low back pain in Adults. *Neuromodulation*, *17*(S2), 3–10.

Markolf, K. K. L., & Morris, J. J. M. (1974). The structural components of the intervertebral disc. *The Journal of Bone & Joint Surgery*, *56*(4), 675–687.

Naserkhaki, S., Arjmand, N., Shirazi-Adl, A., Farahmand, F., & El-Rich, M. (2018). Effects of eight different ligament property datasets on biomechanics of a lumbar L4-L5 finite element model. *Journal of Biomechanics*, *70*, 33–42.

Newell, N., Little, J. P., Christou, A., Adams, M. A., Adam, C. J., & Masouros, S. D. (2017). Biomechanics of the human intervertebral disc: A review of testing techniques and results. *Journal of the Mechanical Behavior of Biomedical Materials*, *69*, 420–434.

O'Leary, S. A., Link, J. M., Klineberg, E. O., Hu, J. C., & Athanasiou, K. A. (2017). Characterization of facet joint cartilage properties in the human and interspecies comparisons. *Acta Biomaterialia*, *54*, 367–376.

Oxland, T. R. (2016). Fundamental biomechanics of the spine-What we have learned in the past 25 years and future directions. *Journal of Biomechanics*, *49*(6), 817–832.

Palepu, V., Kodigudla, M., & Goel, V. K. (2012). Biomechanics of Disc Degeneration. *Advances in Orthopedics*, *2012*(6), 17.

Panjabi, M. M., Oxland, T. R., I., Y., & Crisco, J. J. (1994). spinal disorders, trauma. Clinical. *The Journal of Bone and Joint Surgery*, *76*(3), 413–424.

Panjabi, M. M., Oxland, T., Takata, K., Goel, V., Duranceau, J., & Krag, M. (1993). Articular facets of the human spine:Quantitative three-dimensional anatomy. *Spine*, *18*(10), 1298–1310.

Park, W. M., Kim, K., & Kim, Y. H. (2013). Effects of degenerated intervertebral discs on intersegmental rotations, intradiscal pressures, and facet joint forces of the whole lumbar spine. *Computers in Biology and Medicine*, *43*(9), 1234–1240.

Patrick, N., Emanski, E., & Knaub, M. A. (2014). Acute and chronic low back pain. *Medical Clinics of North America*, *98*(4), 777–789.

Patwardhan, A. G. (1999). A Follower Load Increases the Load-Carrying Capacity of the Lumbar Spine in Compression.

Peng, T., Pérez, A., & Pettee Gabriel, K. (2018). The Association Among Overweight, Obesity, and Low Back Pain in U.S. Adults: A Cross-Sectional Study of the 2015 National Health Interview Survey. *Journal of Manipulative and Physiological Therapeutics*, *41*(4), 294–303.

Pintar, F. A. (1992). Biomehcanical properties of human lumbar ligaments. *Journal of Biomechanics*, *25*(11), 1351–1356.

Ranu, H. (1990). Ranu - 1990 - Measurement of pressures in the nucleus and within the annulus of the human spinal disc due to extreme loading, *204*, 141–146.

Ritzel, H., Amling, M., Pösl, M., Hahn, M., & Delling, G. (1997). The thickness of human vertebral cortical bone and its changes in aging and osteoporosis: A histomorphometric analysis of the complete spinal column from thirty-seven autopsy specimens. *Journal of Bone and Mineral Research*, *12*(1), 89–95.

Roffey, D. M., Ashdown, L. C., Dornan, H. D., Creech, M. J., Dagenais, S., Dent, R. M., & Wai, E. K. (2011). Pilot evaluation of a multidisciplinary, medically supervised, nonsurgical weight loss program on the severity of low back pain in obese adults. *Spine Journal*, *11*(3), 197–204.

Rohlmann, A. (2001). Loads on an internal spinal fixation device during sitting. *Journal of Biomechanics 34*, *125*(April), 989–993.

Rohlmann, A., Burra, N. K., Zander, T., & Bergmann, G. (2007). Comparison of the effects of bilateral posterior dynamic and rigid fixation devices on the loads in the lumbar spine: A finite element analysis. *European Spine Journal*, *16*(8), 1223–1231.

Rohlmann, A., Mann, A., Zander, T., & Bergmann, G. (2009). Effect of an artificial disc on lumbar spine biomechanics: A probabilistic finite element study. *European Spine Journal*, *18*(1), 89–97.

Rohlmann, A., Neller, S., Claes, L., Bergmann, G., & Wilke, H. (2001). Rohlmann_2001.pdf, *26*(24), 557–561.

Rolin, O. Y., & Carter, W. E. (2019). *5 – Biomechanics of the Spine*. *Atlas of Orthoses and Assistive Devices* (Fifth Edit, Vol. 2). Elsevier Inc.

Schmidt, H., Heuer, F., Drumm, J., Klezl, Z., Claes, L., & Wilke, H. J. (2007). Application of a calibration method provides more realistic results for a finite element model of a lumbar spinal segment. *Clinical Biomechanics*, *22*(4), 377–384.

Schulte, T. L., Hurschler, C., Haversath, M., Liljenqvist, U., Bullmann, V., Filler, T. J., … Hackenberg, L. (2008). The effect of dynamic, semi-rigid implants on the range of motion of lumbar motion segments after decompression. *European Spine Journal*, *17*(8), 1057–1065.

Silva-Correia, J., Correia, S. I., Oliveira, J. M., & Reis, R. L. (2013). Tissue engineering strategies applied in the regeneration of the human intervertebral disk. *Biotechnology Advances*, *31*(8), 1514–1531.

Sparks, C. L., Liu, W. C., Cleland, J. A., Kelly, J. P., Dyer, S. J., Szetela, K. M., & Elliott, J. M. (2017). Functional Magnetic Resonance Imaging of Cerebral Hemodynamic Responses to Pain Following Thoracic Thrust Manipulation in Individuals With Neck Pain: A Randomized Trial. *Journal of Manipulative and Physiological Therapeutics*, *40*(9), 625–634.

Stokes, I. A. F. (1987). Surface strain on human intervertebral discs. *Journal of Orthopaedic Research*, *5*(3), 348–355.

Urban, J. P., & Roberts, S. (2003). Degeneration of the intervertebral disc. *Arthritis Research & Therapy*, *5*(3), 120.

Violante, F. S., Mattioli, S., & Bonfiglioli, R. (2015). *Low-back pain*. *Handbook of Clinical Neurology* (1st ed., Vol. 131). Elsevier B.V.

Wang, L., Zhang, B., Chen, S., Lu, X., Li, Z., & Guo, Q. (2016). A Validated Finite Element Analysis of Facet Joint Stress in Degenerative Lumbar Scoliosis. *World Neurosurgery*, *95*, 126–133.

Waongenngarm, P., Areerak, K., & Janwantanakul, P. (2018). The effects of breaks on low back pain, discomfort, and work productivity in office workers: A systematic review of randomized and non-randomized controlled trials. *Applied Ergonomics*, *68*(April 2017), 230–239.

Wilke, H.-J., & Volkheimer, D. (2018). *Basic biomechanics of the spine*. *Neurosurgery* (Vol. 7). Elsevier Ltd.

Yassi, A., & Lockhart, K. (2013). Work-relatedness of low back pain in nursing personnel: A systematic review. *International Journal of Occupational and Environmental Health*, *19*(3), 223–244.

Zahari, S. N., Latif, M. J. A., Rahim, N. R. A., Kadir, M. R. A., & Kamarul, T. (2017). The Effects of Physiological Biomechanical Loading on Intradiscal Pressure and Annulus Stress in Lumbar Spine: A Finite Element Analysis. *Journal of Healthcare Engineering*, *2017*, 1–8.

Zhang, Z., Fogel, G. R., Liao, Z., Sun, Y., & Liu, W. (2018). Biomechanical analysis of lumbar interbody fusion cages with various lordotic angles: a finite element study. *Computer Methods in Biomechanics and Biomedical Engineering*, *21*(3), 247–254.

Zhong, Z. C., Wei, S. H., Wang, J. P., Feng, C. K., Chen, C. S., & Yu, C. H. (2006). Finite element analysis of the lumbar spine with a new cage using a topology optimization method. *Medical Engineering and Physics*, *28*(1 SPEC. ISS.), 90–98.